SPECIATION AND REACTIVITY OF PHOSPHORUS AND ARSENIC IN MID-ATLANTIC SOILS

by

Audrey Gamble

A dissertation submitted to the Faculty of the University of Delaware in partial fulfillment of the requirements for the degree of Doctor of Philosophy in Plant and Soil Sciences

Spring 2017

SPECIATION AND REACTIVITY OF PHOSPHORUS AND ARSENIC IN MID-ATLANTIC SOILS

by

Audrey Gamble

Approved: _____
Robert E. Lyons, Ph.D
Interim Chair of the Department of Plant and Soil Sciences

Approved: _____
Mark Rieger, Ph.D.
Dean of the College of Agriculture and Natural Resources

Approved: _____
Ann Ardis, Ph.D.
Senior Vice Provost for Graduate and Professional Education

I certify that I have read this dissertation and that in my opinion it meets the academic and professional standard required by the University as a dissertation for the degree of Doctor of Philosophy.

Signed: _____

Donald Sparks, Ph.D.
Professor in charge of dissertation

I certify that I have read this dissertation and that in my opinion it meets the academic and professional standard required by the University as a dissertation for the degree of Doctor of Philosophy.

Signed: _____

Amy Shober, Ph.D.
Member of dissertation committee

I certify that I have read this dissertation and that in my opinion it meets the academic and professional standard required by the University as a dissertation for the degree of Doctor of Philosophy.

Signed: _____

Paul Northrup, Ph.D.
Member of dissertation committee

I certify that I have read this dissertation and that in my opinion it meets the academic and professional standard required by the University as a dissertation for the degree of Doctor of Philosophy.

Signed: _____

Dalton Abdala, Ph.D.
Member of dissertation committee

ACKNOWLEDGMENTS

TABLE OF CONTENTS

Appendix

LIST OF TABLES

LIST OF FIGURES

ABSTRACT

Phosphorus (P) and arsenic (As) are chemically similar elements with widely different impacts on the environment. Phosphorus is an essential element for crop growth and a widely-applied fertilizer to agricultural soils, but can act as a pollutant when excess P erodes or leaches into water sources, adversely affecting water quality. Arsenic is a known carcinogen that occurs naturally and anthropogenically in soils and can pose significant risk to human health. An understanding of fundamental soil P and As chemistry is necessary to understand cycling and bioavailability of these elements in the environment. Synchrotron-based X-ray absorption near edge spectroscopy (XANES) and X-ray fluorescence (XRF) techniques are used in the current study to determine speciation of P and As in soils from the Mid-Atlantic. This paper has three primary objectives: 1) examine soil P speciation (chemical forms) using novel synchrotron-based micro-focused XANES (μ-XANES) techniques; 2) comparatively assess P desorption potential in Mid-Atlantic soils based on soil chemical and physical properties; and 3) assess the toxicity and bioavailability of As in historically-contaminated orchard soils, where lead arsenate was applied. In this study, XAS and XRF techniques (objective 1) have identified calcium phosphates, Fe phosphates, Al-sorbed P, and Fe-sorbed P in soils. Our study demonstrates the value in pairing XRF and XAS studies to evaluate P speciation *in situ* for soils. Sequential extractions indicate that P is primarily associated with iron (Fe) and (Al) in the evaluated soils, and batch desorption demonstrates that soils with high amorphous Fe- and Al-oxide content are less vulnerable to desorption (objective 2). Results from sequential extracts were not representative of major species identified with XAS techniques, and could signify that P speciation is more easily detected for discrete, P-rich particles with μ-XANES. Bioavailability and speciation

studies to assess soil As toxicity in legacy orchard soils (objective 3) indicate less than 22% of total As is bioavailable at all previous orchard locations. All As appears to be in the less-toxic As(V) form based on XAS analysis. Arsenic is relatively immobile in background electrolyte solutions, but phosphate concentration increases As mobility in contaminated soils. These studies demonstrate the importance of synchrotron-based methods to evaluate P and As speciation in soil.

Chapter 1

LITERATURE REVIEW

Phosphorous (P) and arsenic (As) react similarly in the environment due to their similar atomic radii and electron configurations. Both elements occur predominantly as oxyanions in the +V oxidation state in oxic soils. Both arsenate and phosphate are adsorbed strongly to soil minerals with variable-surface charge via inner-sphere complexation (Fendorf et al., 1997; Yang et al., 2002; Beak et al., 2006; Arai and Sparks, 2007). Iron (Fe) and aluminum (Al) oxides are often the most important sorbents of P and As in soils, and the affinity for metal oxides to sorb these oxyanions tends to increase in low pH soils (Violante and Pigna, 2002; Dixit and Hering, 2003; Arai and Sparks, 2006). Phosphate and arsenate are known to compete for sorption sites on metal oxide surfaces (Violante and Pigna, 2002; Neupane et al., 2014)

Although chemically similar, P and As have very different roles in the environment. Phosphorus is an essential plant nutrient that is needed for plant growth, but can acts as a pollutant when excess P runs off into surface waters. Elevated levels of P in aquatic systems can cause excessive phytoplankton growth, decreased levels of dissolved oxygen, and an overall reduction in water quality. As P pollution from point sources has been reduced over the past two decades, the relative contribution from nonpoint sources has increased. For example, agriculture is currently the largest source of nonpoint pollution entering the Chesapeake Bay, accounting for an estimated 50% of P entering the watershed (Russell et al., 2008). Goals set to remove Chesapeake Bay

1

from the United States EPA impaired water list by 2010 were not met (EPA, 2010). However, many states have made significant progress in reducing P loss from agriculture. By understanding the speciation and reactivity of P in agricultural soils, best management practices to increase P use efficiency and reduce P pollution in areas such as the Chesapeake Bay watershed can be developed.

Arsenic is a known toxin and carcinogen, and elevated levels of As in soil can pose severe risk to human and environmental health. Soil As contamination can result from both anthropogenic and geogenic inputs. In fact, As release from naturally-occurring sediments in south and southeast Asia has exposed millions of people to toxic level of As (Polizzotto et al., 2008) and is often considered the largest mass poisoning in human history (Yu et al., 2003). In Delaware, lead arsenate was a commonly used pesticide in fruit tree orchards from the 1890s to 1940s (Udovic and McBride, 2012). Soil As concentrations exceeding 100 mg kg^{-1} persist in former peach and apple orchards in the Pacific Northwest, New York State, and Pennsylvania (Davenport and Peryea, 1991; Jones and Hatch, 1937; Merwin et al., 1994), falling far above the EPA established soil As screening levels of 0.4 mg kg^{-1}. Delaware was among the leading producers of fruit tree orchards in the late 1800s (Hedrick et al., 1917), and elevated levels of As likely exist in many former orchards in Delaware. Knowledge the speciation and reactivity of As is important to determine remediation strategies necessary to limit toxicity of As in contaminated soils.

1.1   Phosphorus Speciation

An understanding of the mechanisms by which P is retained in soils can give further insights into desorption, mineralization, and dissolution processes which govern

P mobility in soils. The low concentration of P relative to other soil components (e.g. Si, Al, Fe) increases difficulty in direct spectroscopic methods to identify P speciation at the molecular level (Piersynski et al., 1990). Early studies using adsorption isotherms (Heylar et al., 1976) and surface complexation modeling (Goldberg and Sposito, 1984a,b) have demonstrated that phosphate forms inner-sphere complexes on metal oxide surfaces. Inner-sphere complexation is not affected by ionic strength. Therefore, changes in phosphate adsorption isotherm data with varying ionic strength can be used to predict outer- versus inner-sphere complexation. Arai and Sparks (2001) observed no dependence of phosphate adsorption on ionic strength (0.01 to 0.8 M NaCl) below pH 7.5, suggesting the formation of inner-sphere complexes on ferrihydrite surfaces. Phosphate adsorption to oxide surfaces through inner-sphere complexation also results in a decrease in charge of the mineral surface. Therefore, electrophoretic mobility measurements can also be used to assess phosphate sorption mechanisms to mineral and oxide surfaces (Bleam et al., 1991). Tejedor-Tejedor and Anderson (1990) observed a decrease in isoelectric point pH values with increasing phosphate loadings onto goethite, indicating the formation of inner-sphere complexes. Although inner-sphere complexation can be inferred from solution data, direct evidence of P speciation is not provided using these methods.

1.1.1 Fourier Transform Infrared Spectroscopy

Fourier transform infrared (IR) spectroscopy has been used previously to assess speciation of P adsorbed to Fe- and Al-oxide surfaces in pure mineral systems, but poses difficulty for determining P speciation *in situ* for soils (Piersynski et al., 1990). The spectra of other soil components, such as spectral bands resulting from bending

3

vibrations for Al-OH-Al bonds in aluminosilicate materials and stretching vibrations for Si-O-Si bonds in silicate minerals, commonly overlap with spectral features for phosphate (Kizewski et al., 2011). Studies using IR spectroscopy to determine phosphate adsorption mechanisms in pure mineral systems have led to inconclusive results. For example, formation of monodentate mononuclear (Tejedor-Tejedor and Anderson, 1990; Persson et al., 1996) and bidentate binuclear (Parfitt et al., 1975; Tejedor-Tejedor and Anderson, 1990; Luengo et al., 2006) inner-sphere surface complexes have been observed for phosphate sorbed to goethite at low pH (≤ 6). Arai and Sparks (2001) also suggest the formation inner-sphere complexes for phosphate sorption to ferrihydrite at pH 6 using FTIR.

1.1.2 Nuclear Magnetic Resonance Spectroscopy

Nuclear magnetic resonance (NMR) spectroscopy measures the resonance between a magnetic field and atomic nuclei possessing magnetic properties. This techniques poses difficulty for measuring P speciation in unaltered soils, since Fe and manganese (Mn), which are ubiquitous in soils, also have nuclei with magnetic properties and can create artifacts in NMR spectra. However, NMR has been frequently used to determine organic P forms in soil extracts. Soils are typically extracted with a combination of sodium hydroxide (NaOH) and ethylenediaminetetraacetic acid (EDTA) prior to NMR analysis; organic P species of phosphonates, orthophosphate monoesters, and orthophosphate diesters have been detected in extracts (Cade-Menun and Liu, 2013).

Solid-state NMR has been used to characterize phosphate bonding mechanisms in pure mineral systems not containing Fe or Mn. Bleam et al. (1991) used solid state

NMR to provide evidence that inner-sphere complexation occurs on boehmite surfaces. Recently, Li et al. (2013) conducted a study which compared solid-state NMR spectra for samples to spectra generated by computational models to examine sorption mechanism for phosphate on Al oxides. They evaluated phosphate sorption over a range of variables including pH (4-10), P concentration (0.1-10 mM), ionic strength (0.001-0.5 M), and reaction time (15 min- 22 d) for boehmite but did not see a large effect of these variables on bonding mechanism. They suggest the formation of monodentate mononuclear inner-sphere complexes under surface wetting conditions. Li et al. (2013) also compared phosphate sorption on various Al oxides including gibbsite, bayerite, boehmite, corundum, and γ-alumina. They suggest that a bidentate binuclear inner-sphere complex is the dominant mechanism for P sorption based on ^{31}P solid-state NMR techniques, but the ^{31}P NMR spectra varied according to adsorbent. These data suggests that NMR was not sensitive enough to assess the lesser components of phosphate sorption.

1.1.3 X-Ray Absorption Near Edge Structure Spectroscopy

Phosphorus K-edge X-ray absorption near edge structure (XANES) has been used previously to characterize the chemical forms of P in soils (Beauchemin et al., 2003; Sato et al., 2005) and in poultry litter (Peak and Sparks, 2002; Sato et al., 2005; Shober et al., 2006) for "bulk" samples. "Bulk" sample analysis is used to measure the average P speciation of soil with a defocused beam (Kar et al., 2012). XANES spectra exhibit distinct characteristics based on the chemical environment on P in a sample. A primary fluorescence peak of the P K-edge XANES spectra is observed at approximately 2152 eV, a result of decay of an electron into the 1s shell after X-rays have excited an electron

from the 1s shell (Brandes et al., 2007). Stability of the monochromator affects the peak position, and it is important to ensure the stability with known standards to ensure that the white line does not shift during XANES analysis (Brandes et al., 2007).

Calcium phosphate minerals have a characteristic post-edge shoulder from approximately 2 to 6 eV above the P K-edge of XANES spectra (Hesterberg et al., 1999 Ingall et al., 2011). Potassium phosphates can also produce a post-edge shoulder in XANES spectra, but the shoulder has a lower relative peak height compared to the post-edge for Ca phosphate. In addition, XANES for potassium phosphate salt do not have distinct secondary peak features (Brandes et al., 2007). A slight downward shift (appr. 0.2-0.6 eV) has also been observed for Ca phosphates when compared to Fe- and Al-phosphates (Lombi et al., 2006). Bulk XANES analysis has been used to distinguish Ca phosphate minerals apatite and brushite in soils after fertilizer application (Kar et al., 2012).

Spectra for phosphate bound to oxidized Fe [Fe(III)] display a pre-edge feature approximately -2 to -4 eV relative to the P K-edge, with the pre-edge feature becoming more distinct dependent upon the number of Fe atoms to which it is bound (Khare et al., 2004; Brandes et al., 2007). For example, Fe phosphate mineral species have a more defined pre-edge than phosphate sorbed to Fe(III) oxides (Hesterberg et al., 1999; Shober et al., 2006). The pre-edge feature is not as defined for P bound to reduced Fe species. Early studies using P K-edge XANES in the environmental sciences used intensity of the pre-edge for Fe(III)-associated P to examine the distribution of phosphate in binary mineral systems (Khare et al., 2004; Khare et al., 2005). For example, Khare et al. (2004) used XANES to distinguish phosphate sorbed to boehmite from phosphate sorbed to ferrihydrite in batch reactions with varying degrees of phosphorus loading at pH 6. Abdala et al. (2015c) used P K-edge XANES to demonstrate that long term (>10 yr)

6

manure application resulted in a decrease in crystalline Fe-bound P species and an increase in amorphous Fe-bound species compared to unaltered soils by measuring the intensity of the pre-edge feature. In studies examining phosphate sorption to ferrihydrite at pH 4 and 7.5, Arai and Sparks (2007) observed an increased intensity of the pre-edge feature over time from 5 min to 11 months; this increased intensity was likely a result of an increase in the number of phosphate atoms sorbed the Fe oxide surface through inner-sphere complexation. Pre-edge features can also occur for K, Mn, and Ni phosphates (Brandes et al., 2007), but these species are less concentrated in soils.

XANES spectra for organic P species tend to have less distinct features. Brandes et al. (2007) observed identical peak positions for organic standards including phytic acid, phosphatidylethanolamine, ATP, O-phosphoryl ethanolamine, and phenyl phosphate. However, they were able to discern reduced P compounds based on a 1 eV downward shift in primary peak position in compounds such as 2-aminoethylphosphonic acid. Studies have not been very successful in determining organic P speciation in soil samples, and it is common to report organic P as a general species which can be differentiated from inorganic P by its broadened white line peak (Peak and Sparks, 2002; Kar et al., 2012). Phytic acid generally contributes to over 50% of total organic P in soil (Arai and Sparks, 2007) and is a common organic standard to include during data processing. Although specific organic P species have not been reliably detected in soils, organic species such as phytic acid, polyphosphate, and monoesters have been observed in poultry litter samples due to the increased organic P concentration in manures (Seiter et al., 2008).

Self-absorption of fluorescence is a common problem encountered during P K-edge XANES analysis due to changes in penetration depth of incident X-rays and is

difficult to avoid at the low energy (~2150 eV) of incident X-rays at the P K-edge. Self-absorption primarily results in a distortion of peak amplitude but does not change the position of features in the XANES spectra, and can result in high heterogeneity in the results methods for analyzing XANES spectra such as principal component analysis (PCA) and linear combination fitting (LCF). Some studies have used total electron yield (TEY) detectors to overcome effects of self-absorption in standards or soil samples concentrated in P (Okude et al., 1999; Toor et al., 2006).

In addition to self- absorption effects on P K-edge XANES, low signal to-noise ratio and accurate choice of standards create difficulty in processing XANES data. Over 150 P minerals are known to exist in soil (Arai and Sparks, 2007), and a variety of sorbed and organic P also exist in soils. A robust standards library is necessary to account for all possible soil P species. LCF fitting may not be sensitive enough to distinguish P species for XANES spectra that show only slight differences. Shober et al. (2006) observed that when aqueous phosphate was substituted for Al-sorbed P using LCF, fitting results only changed by approximately 20 percent. To measure the accuracy of LCF fitting, Ajiboye et al. (2007) performed LCF analysis on P K-edge XANES for known binary mixtures of variscite, phosphosiderite, and apatite. Each of these minerals have distinct XANES features, representing an ideal system for LCF. To avoid self-absorption, mixtures were diluted in boron nitride before bulk XANES analysis. They observed up to ~40% error in mixture containing known amounts of phosphosiderite and apatite; the goodness-of-fit calculated for this fit was high, even though the measured accuracy was low. The accuracy of LCF analysis increased with increasing proportions of apatite (Ajiboye et al., 2007), likely due to the distinct post-edge shoulder and secondary peaks observed for apatite. Error for mixtures of apatite and variscite ranged from 0.8-17%, indicating that in binary mixtures with known composition, LCF can be useful. However, for samples

containing components with less-distinct features, particularly in heterogenous media such as soil, the accuracy of LCF fitting is expected to decrease.

1.1.4   Micro- X-Ray Absorption Near Edge Structure Spectroscopy

A higher degree of certainty for P speciation can be achieved by focusing the X-ray beam to a size similar to that of soil particles. The high resolution of micro-focused XANES is useful to examine P speciation in individual particles or aggregates, and limits the number of P species detected in XANES spectra. To achieve spatially-resolved P speciation, micro-focused X-ray fluorescence (μ-XRF) can map the distribution of elements of interest for P speciation (i.e., P, Al, Fe, Ca, Si) with high spatial resolution (≤ 10 μm). Following μ-XRF analysis, micro-focused XANES (μ-XANES) spectra can be used to examine the bonding environment of P. Micro-XANES analysis is advantageous that fewer forms of P are detected in XANES spectra because of the smaller beam size.

Very few researchers have used μ-XRF in combination with μ-XANES to examine P speciation in environmental samples. This technique has been applied to study marine sediments (Brandes et al., 2007; Giguet-Covex et al., 2013) and speleothems (Frisia et al., 2012), but have not been widely applied to soils. Lombi et al. (2006) and Schefe et al. (2011) used spatially-resolved XANES studies to compare the effectiveness of fertilizers applied to soils in laboratory settings at high concentrations. Giguex-Covex et al. (2013) studied P speciation during soil genesis by collecting μ-XANES spectra of lake sediments for which soil development history during the Holocene has been well-studied. It should be noted that the use of scanning transmission spectroscopy paired with energy dispersive X-ray analysis has also been used previously to examine correlation of P with

Al, Si, Ca, and Fe in soil particles, but this technique cannot determine information regarding the bonding environment of P (Piersynski et al, 1990; Arai and Livi, 2013).

Calcium phosphate minerals are the most frequently-identified P species identified in these studies, due to the distinct post-edge shoulder and secondary peaks which are observed in XANES spectra (Lombi et al., 2006; Brandes et al., 2007; Giguex-Covex et al., 2013). Lombi et al. (2006) used nano-focused XANES to confirm P was primarily associated with Ca after fertilization in calcareous soils. Similar to bulk XANES studies, organic P species are difficult to distinguish in μ-XANES analysis.

Schefe et al. (2011) used micro-focused XANES to complete speciation of fertilizer-amended soils with approximately 1700 mg kg^{-1} P. They concluded that in soils with 100 mM P addition, P speciation was likely complex, but small contributions of Mg-bound P and Fe-bound P likely occur. Assumed that higher relative concentration of Al and Si compared to P made it difficult to find differences in P speciation in various P/carboxylic acid treatments, despite these treatments having an effect on P concentration. Although they saw increases in total P XRF intensity, they were not able to obtain quality XANES spectra.

1.1.4.1   Sample Preparation

A variety of sample preparation techniques have been used for P K-edge X-ray absorption analysis of soils. The most common techniques include loose powder, pressed-pellet, and polished thin-section preparation. Loose powder provides the most unaltered type of sample, but does not provide a flat surface for X-ray spectroscopy. Shadowing by larger particles can reduce fluorescence signal and omit finer particles from analysis. To prepare a loose powder sample for X-ray analysis, only a few

milligrams of sample is needed. It is common to sieve soils to a fine powder (~125-250 μm) to reduce shadowing and increase P concentration. Typical X-ray transparent tapes, such as Kapton, are not recommended for P K-edge analysis since they may contain P impurities. Instead, hydrocarbon tape is preferred for mounting soil samples.

A pressed pellet provides a flat surface for analysis, but may not accurately represent the distribution of P in a sample since this technique preferentially sorts particles. For instance, smaller particles may congregate at the surface of pressed pellets. The pressure applied to form a pressed-pellet may alter the configuration of soil aggregates or particles, and the heat load generated during preparation has potential to alter P speciation. Giguex-Covex et al. (2013) used pressed pellet samples of 500-μm thickness wrapped in a hydrocarbon film for μ-XANES analysis.

A polished thin-section also provides a flat surface does not preferentially sort particles. The flat surface of a polished section reduces scatter compared to powder. Thin-sectioning is the most ideal preparation method to obtain a good P signal but is the most altered type of sample. Incorporation of soil into a resin to produce a polished section has potential to chemically alter P speciation. Prior to thin-sectioning, soils are typically loaded into an epoxy resin, sectioned, polished, and mounted to a glass slide. High-purity quartz slides are recommended for mounting to avoid P contamination. Thin sections of 100-μm (Schefe et al., 2010) and 2.5-μm (Lombi et al., 2006) thickness have been previously used for μ-XANES analysis at the P K-edge.

1.1.4.2   Data Collection

Prior to μ-XANES analysis, it is necessary to scan the soil sample using X-ray fluorescence to determine the location of P hotspots. Samples and detectors are be kept

in He environment during analysis. Minimum spatial resolution for XRF analysis is dependent upon beamline capabilities. Previous micro-XANES studies have used spatial resolutions at micron (Schefe et al., 2010; Monnier et al., 2011) or sub-micron (Lombi et al., 2006; Brandes et al., 2007; Giguex-Covex et al., 2013) scales. Kirkpatrick-Baez mirrors or zone plates are frequently used to achieve micro-focused beam sizes. The excitation energy for XRF maps is kept above the P K-edge at approximately 2200 to 2500eV to detect P, Al, Si, and Mg fluorescence (Schefe et al., 2010; Monnier et al., 2011). Since Ca and Fe are important elements associated with P in soils, it is useful to examine P correlation with Fe and Ca in samples. Tender energy beamlines can occasionally collect fluorescence at the Ca K-edge, but P fluorescence signal is weakened at the higher energy required for Ca analysis. Monnier et al. (2011) was able to collect Fe fluorescence at the Fe Lα-edge in a concentration Fe sample, but the signal tends to be too weak to detect Fe fluorescence at the Lα-edge for heterogeneous soil mixtures (Schefe et al., 2011). If samples are prepared in a manner which allows the same region to be measured at separate beamlines, a comparison of μ-XRF maps from a tender energy imaging beamline can be compared to maps from a high-energy (4.5-24 keV) imaging beamline to assess the elemental distribution of P with Fe and Ca. Consultation with the beamline scientist is recommended to determine the beam size and dwell-time best-suited for a given experiment.

XANES spectra are typically collected at the energy region nearest the P K-edge (~2140 to 2160 eV) with an energy step-size of 0.2 to 0.25 eV (Lombi et al., 2006; Brandes et al., 2007; Giguex-Covex et al., 2013). Silicon drift detectors are often preferred detectors for data collection in fluorescence mode. Multiple XANES spectra are usually collected and averaged at each hotspot to reduce signal-to-noise ratio. The number of scans required will depend on the P species, concentration, and beamline

quality; this number has ranged from two to six spectra for each hotspot in previous studies (Lombi et al., 2006; Schefe et al., 2010; Giguex-Covex et al., 2013).

1.1.4.3 Data Processing

Software to examine X-ray fluorescence maps such as Sam's MicroAnalysis Toolkit (Webb, 2005) can be used to map the distribution of fluorescence for elements of interest. Fluorescence for each element is normalized to the highest fluorescence counts; areas with the highest fluorescence counts are represented in maps. Correlation analyses can also be performed in such software to assess the association of P with elements of interest.

The high resolution of μ-focused XANES limits the number of P species analyzed in XANES spectra and it can be assumed that only one or two forms of P are detected in a XANES spectra. By using a "fingerprinting" method, in which features in μ-XANES sample spectra are compared to those of known standards, P speciation can be identified (Brandes et al., 2007). Extensive libraries of XANES spectra for mineral, sorbed, and organic P species can be found in Ingall et al., (2011), Prietzel et al., (2016), and Brandes et al, (2007), respectively. Giguex-Covex et al. (2013) used LCF to assess speciation if the fingerprinting method suggested that more than one species was present. However, self-absorbance is common in μ-XANES analysis at the P K-edge (Lombi et al., 2006; Schefe et al., 2011), and LCF should be used with precaution. Schefe et al. (2011) determined that self-absorption resulted in a 15% decrease in amplitude for some standard P minerals. Slight differences have been observed between XANES spectra collected at a nano-fucused beamline compared to bulk XANES spectra for standards, likely due to self-absorption. (Lombi et al., 2006). Dilutions in X-ray

13

transparent materials can be run to determine if higher concentration samples dampen spectra for standard species, but it is not possible to dilute P in localized P-rich particles. Therefore, it is best to make inferences regarding P speciation based on the position and separation of peak features of μ-XANES spectra, rather than peak amplitude.

The quality of spectra varies dependent on the localized P concentration in an area of interest. In general, a higher signal-to-noise ratio is expected in μ-XANES compared to bulk XANES analysis due to the smaller size of the X-ray beam. It should be noted that soils with low P concentration may be challenging to analyze with μ-XANES. Schefe et al. (2011) report that signal-to-noise ratio was too low in μ-XANES spectra to determine P in untreated soils.

1.1.5 Extended X-Ray Absorption Fine Structure Spectroscopy

Extended X-ray absorption fine structure (EXAFS) spectroscopy identify more specific P speciation information by determining nearest-neighbor identity, bond distances, and coordination number of P. The use of EXAFS at the P K-edge for environmental samples is relatively novel. Fluorescence yield decreases with decreasing atomic number, making it difficult to obtain adequate signal to measure P EXAFS, particularly in dilute, environmental samples. Rouff et al. (2009) demonstrated that EXAFS can be used to distinguish protonation state of phosphate in aqueous samples. Abdala et al. (2015a) and Abdala et al. (2015b) have used EXAFS to distinguish surface precipitates and surface complexation mechanisms of P on goethite. They observed the formation of bidentate binuclear, bidentate mononuclear, and monodentate mononuclear bonding configurations on goethite and an increasing formation of

bidentate binuclear bonding configuration with longer reaction times and lower surface loading.

When examining the effect of surface coverage on bonding configuration of phosphate on goethite, Abdala et al. (2010a) observed calculated P-O bond distances of 1.51 to 1.53 Å from $\chi(k)$ spectra. They report a multiple scattering peak occurs at approximately 2.75 to 2.78 Å. The P-Fe distance were approximately 2.83 to 2.87 Å for the bidentate mononuclear, 3.2 to 3.3 Å for the bidentate binuclear, and 3.6 Å for the monodentate mononuclear configuration. Abdala et al. (2010a) also observed the formation of surface precipitates can when monolayer coverage was exceeded on the goethite surface. With technological advances, it may be possible to identify phosphate bonding mechanisms for other P species.

1.2   Phosphorus Retention

Phosphorus retention in soils is regulated by precipitation and dissolution of mineral P, immobilization and mineralization of organic P, and adsorption and desorption of sorbed P. Desorption of P is characterized by an initial rapid reaction, followed by a slow desorption reaction (Kuo and Lotse, 1973; McGechan et al., 2002; Arai et al., 2007). The retention of P is largely dependent upon chemical and mineralogical characteristics of soils. Amorphous Fe- and Al-oxide, organic matter, and Ca contents are each important contributors to P retention (Arai and Sparks, 2007). Strong retention of phosphate via inner-sphere complexation on Fe- and Al-oxides is known to limit amount of available P in acidic soils. Slow P desorption processes can be attributed to the higher activation energy created when inner-sphere complexation occurs.

15

Phosphate sorption to metal oxide surfaces is known to increases with decreasing pH (Bleam et al., 1991; Arai and Sparks, 2001). When the pH of bulk soil solution is lower than the point of zero charge (PZC) of the mineral surface, a net positive surface charge attracts negatively charged phosphate ions. Acidity can decrease the availability of P to crops dues to an increase in number of sorption sites on oxide and aluminosilicate and metal oxide particles. P can also have low solubility in calcareous soils due to the low solubility of Ca phosphate minerals.

Organic matter content is also important in controlling P retention. Kang et al. (2009) found that high OM (>49 g kg^{-1} soil) content decreased the affinity for Fe- and Al-oxides to sorb phosphate. Abdala et al. (2015c) demonstrate that the concentration of amorphous Fe- and Al-oxide minerals tends to increase over time in manure-amended soils, providing additional sorption sites for P. Despite increasing concentration of P with manure-amendments, these soils did not have higher soil-test P concentrations; excess P is likely bound to the amorphous Fe- and Al- oxides which are created under manure management.

In continuous-flow column desorption experiments using 10 mM KCl electrolyte solution, the concentration of desorbed P was two times greater for manure-amended soils than adjacent forest soils in the surface horizon in a study by Beauchemin et al. (1999).

Surface precipitation reactions may also occur when sorbed phosphate reacts with dissolved metal ions in soil solution. Traditionally, Langmuir adsorption isotherms have been used to describe P sorption to oxides by attributing different adsorption sites to different linear portions of the Langmuir adsorption model. However, Langmuir isotherms can neither describe a particular adsorption mechanism nor distinguish between adsorption and surface precipitation (Arai and Sparks, 2007).

1.3   Arsenic Speciation

Arsenic (As) is a known toxin and carcinogen, and elevated concentrations of soil As are observed as a result geogenic (Polizzotto et al., 2008) and anthropogenic (Landrot et al., 2012) contamination. In oxic environments, soil As primarily exists in the As(V) oxidation state. Conversely, As is primarily encountered as As(III), the more toxic form of As, under reducing conditions. Even under oxic conditions, small amounts of soil As(V) can reduce to As(III) (Cui and Weng, 2013).

Arsenate speciation is dominated by inner-sphere complexation to metal oxides. Neupane et al. (2014) observed mononuclear and bidentate binuclear surface complexation at the ferrihydrite surface. Fendorf et al. (1997) found that monodentate mononuclear surface complexes dominate arsenate surface complexation to goethite at low surface loadings, while bidentate mononuclear and bidentate binuclear dominate at high surface loadings. Inner-sphere complexation reduces As bioavailability and mobility in soils.

Arai et al. (2006) used synchrotron-based X-ray techniques to determine that As was primarily present as As(V) sorbed to amorphous Fe oxides in sandy soils at a heavily-contaminated site (284 mg As kg^{-1} soil) that had previously contained a lead arsenate production company. Arai et al. (2006) also observed the presence of As sulfide species in a soil sample collected from a contaminated site which periodically experienced reducing conditions. Landrot et al. (2012) observed that As was primarily associated with Al, either as As sorbed to Al-oxide or as an As-Al mineral, in Delaware contaminated soils.

1.4 Arsenic Retention

The retention of soil As is dependent upon a number of factors, including As speciation (form) and soil properties. The reduced form [As(III)] is more mobile than the oxidized form [As(V)] in soil (Cui and Weng, 2013). Iron- and Al-oxide minerals are the typically the most important sorbents of As in soil (Violante and Pigna, 2002; Neupane et al., 2013). It is well-established that As(V) forms inner-sphere complexes to metal oxide surfaces resulting in strong retention by Fe- and Al- oxides in soils under oxic conditions (Fendorf et al., 1997; Yang et al., 2002; Beak et al., 2006). Dixit and Hering (2003) observed sorption of As(V) was preferred on Fe oxide (i.e., goethite, magnetite, and amorphous Fe oxide surfaces at low pH values, while sorption of As(III) was preferred above pH 8. Even at pH ~8, many Fe- and Al-oxides [e.g., α-Al_2O_3, γ-AlOOH, amorphous $Fe(OH)_3$] are positively charged and can retain arsenate. In calcareous soils, arsenate also adsorbs to Ca minerals such as calcite (Goldberg and Glaubig, 1987).

Factors such as pH, redox conditions, soil texture, organic matter (OM) content, and competitive ions also play key roles in As mobility (Merry et al., 1983; Dixit and Hering, 2003; Bradham et al., 2011). Yang et al. (2002) determined that Fe oxide content and pH were the two most important factors controlling soil As bioaccessibility in a survey of 36 soils; the study examined the effect of Fe-oxide content, Mn-oxide content, pH, CEC, carbonate content, organic C content, and particle size on bioaccessibility. In addition to Fe oxide content and pH, Bradham et al. (2011) observed that total Fe and Al content had a large impact on bioaccessible As.

It has been widely-observed that phosphate competes for As(V) sorption sites and can increase As desorption from soils. Neupane et al. (2014) demonstrated that ferrihydrite has a stronger affinity to adsorb arsenate to compared to phosphate at pH 4

and 8. Violante and Pigna (2002) found that more arsenate than phosphate adsorbed to goethite, birnessite, and smectite in equal mixture of phosphate and arsenate. However, higher phosphate compared to arsenate sorption was observed for gibbsite, boehmite, and kaolinite surfaces. Cui and Weng (2013) suggest that arsenate solubility is higher for Al oxides compared to Fe oxides. Although higher ratios of arsenate to phosphate loading have observed for many soil minerals, phosphate addition to decreases total arsenate adsorption to metal oxides (Violante and Pigna, 2002). In lead arsenate-contaminated soils, Peryea et al. (1991) found that approximately 11% of total As was desorbed after 480 h when reacted with 1mM phosphate in batch reactions at pH 6.2. Cui et al. (2013) demonstrated that arsenate was more soluble than phosphate in a study comparing arsenate and phosphate sorption in five soils with a variety of physical and chemical properties, even when soil phosphate concentrations were 10 times higher than added arsenate concentrations.

REFERENCES

Abdala, D.B., P.A. Northrup, F.C. Vicentin, and D.L. Sparks. 2015a. Residence time and pH effects on the bonding configuration of orthophosphate surface complexes at the goethite/water interface as examined by extended x-ray absorption fine structure (EXAFS) spectroscopy. J. Colloid. Interf. Sci. 442:15-21.

Abdala, D.B., P.A. Northrup, Y. Arai, and D.L. Sparks. 2015b. Surface loading effects on orthophosphate surface complexation at the goethite/water interface as examined by extended x-ray absorption fine structure (EXAFS) spectroscopy. J. Colloid. Interf. Sci. 437:297-303.

Abdala, D.B., I. Ribeiro de Silva, L. Vergütz, and D.L. Sparks. 2015c. Long-term manure application effects on phosphorous speciation, kinetics, and distribution in highly weathered agricultural soils. Chemosphere. 119:504-514.

Ajiboye, B., O.O. Akinremi, Y. Hu, and A. Jürgensen. 2008. XANES speciation of phosphorus in organically amended and fertilized Vertisol and Mollisol. Soil Sci. Soc. Am. J. 72:1256-1262.

Arai, Y. and D.L. Sparks. 2001. ATR-FTIR spectroscopic investigation on phosphate adsorption mechanisms at the ferrihydrite-water interface. J. Colloid Interf. Sci. 241:317-326.

Arai, Y., A. Lanzirotti, S.R. Sutton, M. Newville, J. Dyer, and D.L. Sparks. 2006. Spatial and temporal variability of arsenic solid-state speciation in historically lead arsenate contaminated soils. Environ. Sci. Technol. 40:673-679.

Arai, Y., and D.L. Sparks. 2007. Phosphate reaction dynamics in soils and soil components: a multiscale approach. Adv Agron. 94:135-179.

Arai, Y., and K.J. Livi. 2012. Underassessed phosphorus fixation mechanisms in soil sand fraction. Geoderma. 192:422-429.

Beak, D.G., N.T. Basta, K.G. Scheckel, and S.L. Traina. 2006. Bioaccessibility of arsenic(V) bound to ferrihydrite using a simulated gastrointestinal system. Environ. Sci. Technol. 40:1364-1370.

Beauchemin, S., R.R. Simard, and D. Cluis. 1996. Phosphorus sorption-desorption kinetics of soil under contrasting land uses. J. Environ. Qual. 25:1317-1325.

Beauchemin, S., D. Hesterberg, J. Chou, M. Beauchemin, R.R. Simard, and D.E. Sayers. 2003. Speciation of phosphorous-enriched agricultural soils using X-ray absorption near-edge structure spectroscopy and chemical fractionation. J. Environ. Qual. 32:1809-1819.

Bleam, W.F., P.E. Pfeffer, S. Goldberg, R.W. Taylor, and R. Dudley. 1991. A ^{31}P solid-state nuclear magnetic resonance study of phosphate adsorption at the boehmite/aqueous solution interface. Lagmuir. 1991. 1702-1712.

Bradham, K.D., K.G. Scheckel, C.M. Nelson, P.E. Seales, G.E. Lee, M.F. Hughes, B.W. Miller, A. Yeow, T. Gilmore, S.M. Serda, S. Harper, and D.J. Thomas. 2011. Relative bioavailability and bioaccessibility and speciation of arsenic in contaminated soils. Environ. Health Persp. 119:1629-1634.

Cade-Menun, B., and C.W. Liu. 2013. Solution phosphorus-31nuclear magnetic resonance spectroscopy of soils from 2005 to 2013: a review of sample preparation and experimental parameters. Soil Sci. Soc. Am. J. 78:19-37.

Chesapeake Bay Foundation. 2012. The economic argument for cleaning up the Chesapeake Bay and its rivers. Chesapeake Bay Foundation, Annapolis, MD.

Cui, Y., and L. Weng. 2013. Arsenate and phosphate adsorption in relation to oxides composition in soils. Env. Sci. Technol. 47:7269-7276.

Dixit, S. and J.G. Hering. 2003. Comparison of arsenic(V) and arsenic(III) sorption onto iron oxide minerals: implications for arsenic mobility. Environ. Sci. Technol. 37:4182-4189.

Fendorf, S., M.J. Eick, P. Grossl, and D.L. Sparks. 1997. Arsenate and chromate retention mechanisms on goethite. 1. Surface structure. Environ. Sci. Technol. 31:315-320.

Frisia, S., A. Borsato, R.N. Drysdale, B. Paul, A., Grieg, and M. Cotte. 2012. A re-evaluation of the paleoclimatic significance of phosphorous variability in speothems revealed by high-resolution synchrotron micro XRF mapping. Clim. Past. 8:2039-2051.

Giguet-Covex, C., J. Poulenard, E. Chalmin, F. Arnaud, C. Rivard, J.-P. Jenny, and J.-M. Dorioz. 2013. XANES spectroscopy as a tool to trace phosphorus transformation during soil genesis and mountain ecosystem development from lake sediments. Geochim. Cosmochim. Ac. 118:129-147.

Goldberg, S. and G. Sposito. 1984. A chemical model for phosphate adsorption by soils: I. Reference oxide minerals. Soil Sci. Soc. Am. J. 48:772-778.

Goldberg, S., and R.A. Glaubig. 1987. Anion sorption on a calcareous, montmorillonitic soil-arsenic. Soil Sci. Soc. Am. J. 52:1297-1300.

Hesterberg, D., W. Zhou, K.J. Hutchison, S. Beauchemin, and D.E. Sayers. 1999. XAFS study of adsorbed and mineral forms of phosphate. J. Synchrotron Radiat. 6:636-638.

Heylar, K.R., D.N. Munns, and R.G. Burau. 1976. Adsorption of phosphate by goethite. Eur. J. Soil Sci. 27:307-314.

Ingall, E.D., J.A. Brandes, J.M. Diaz, M.D. de Jonge, D. Paterson, I. McNulty, W.C. Elliott, and P. Northrup. 2011. Phosphorus K-edge XANES spectroscopy of mineral standards. J. Synchrotron Ratiat. 189-197.

Kar, G., D. Peak, J.J. Schoenau. 2012. Spatial distribution and chemical speciation of soil phosphorus in a band application. Soil Sci. Soc. Am. J. 76:2297-2306.

Khare, N., D. Hesterberg, S. Beauchemin, and S. Wang. 2004. XANES determination of adsorbed phosphate distribution between ferrihydrite and boehmite in mixtures. Soil Sci. Soc. Am. 68:460-469.

Kizewski, F., Y. Liu, A. Morris, and D. Hesterberg. 2011. Spectroscopic approaches for phosphorus speciation in soils and other environmental systems. J. Environ. Qual. 40:751-766.

Kuo, S., and E.G. Lotse. 1973. Kinetics of phosphate adsorption and desorption by hematite and gibbsite. Soil Sci. 116:400-406.

Landrot, G., R. Tappero, S.M. Webb, and D.L. Sparks. 2012. Arsenic and chromium speciation in an urban contaminated soil. Chemosphere. 88:1196-1201.

Li, W., X. Feng, Y. Yan, D.L. Sparks, and B. Phillips. 2013. Solid-state NMR spectroscopic study of phosphate sorption mechanisms on aluminum (hydr)oxides. Environ. Sci. Technol. 47:8308-8315.

Lombi, E., K.G. Scheckel, R.D. Armstrong, S. Forrester, J.N. Cutler, and D. Paterson. 2006. Speciation and distribution of phosphorus in a fertilized soil: a synchrotron-based investigation. Soil Sci. Soc. Am. J. 70:2038-2048.

Luengo, C., M. Brigante, J. Antelo, and M. Avena. 2006. Kinetics of phosphate adsorption on goethite: comparing batch adsorption and ATR-IR measurements. J. Colloid Interf. Sci. 300:511-518.

Merry, R.H., K.G. Tiller, and A.M. Alston. 1983. Accumulation of copper, lead, and arsenic in some Australian orchard soils. Aust. J. Soil. Res. 21:549-561.

Monnier, J., D. Vantelon, S. Reguer, and P. Dillmann. 2011. X-ray absorption spectroscopy study of the various forms of phosphorous in ancient iron samples. J. Anal. At. Spectrom. 26:885-891.

Okude, N., M. Nagoshi, H. Noro, Y. Baba, H. Yamamoto, and T. A. Sasaki. 1999. P and S K-edge XANES of transition-metal phosphates and sulfates. J. Electron Spectrosc.

Parfitt, R.L., R.J. Atkinson, and Roger C. Smart. 1975. The mechanism of phosphate fixation by iron oxides. Soil Sci. Soc. Am. J. 39:837-841.

Peak, D., J.T. Sims, and D.L. Sparks. 2002. Solid-state speciation of natural and alum-amended poultry litter using XANES spectroscopy. Environ. Sci. Technol. 36:4253-4261.

Persson, P., N. Nilsson, and S. Sjöberg. 1996. Structure and bonding of orthophosphate ions at the iron oxide-aqueous interface. J. Colloid Interf. Sci. 177:263-275.

Piersynski, G.M., T.J. Logan, S.J. Traina, and J.M. Bigham. 1990. Phosphorus chemistry and mineralogy in excessively fertilized soils: Quantitative analysis of phosphorus-rich particles. Soil Sci. Soc. Am. J. 54:1576-1583.

Polizzotto, M.L., B.D. Kocar, S.G. Benner, M. Sampson, and S. Fendorf. 2008. Near-surface wetland sediments as a source of arsenic release to groundwater in Asia. Nature. 454:505-508.

Prietzel, J.,G. Harrington, W. Häusler, K. Heister, F. Werner, and W. Klysuban. 2015. Reference spectra of important adsorbed organic and inorganic phosphate binding forms for soil P speciation using synchrotron-based K-edge XANES spectroscopy. J. Synchrotron Radiat. 23:532-544.

Rouff, A.K., S. Rabe, M. Nachtegaal, and F. Vogel. 2009. X-ray absorption fine-structure study of the effect of protonation and disorder and multiple scattering in phosphate solutions and solids. J. Phys. Chem. 113:6895-6903.

Russell, M.J., D.E. Weller, T.E. Jordan, K.J. Sigwart, and K.J. Sullivan. 2008. Net anthropogenic phosphorus inputs: spatial and temporal variability in the Chesapeake Bay region. Biogeochem. 88:285-304.

Sato, S., D. Solomon, C. Hyland, Q.M. Ketterings, and J. Lehmann. 2005. Phosphorus speciation in manure and manure-amended soils using XANES spectroscopy. Environ. Sci. Technol. 39:7485-7491.

Schefe, C.R., P. Kappen, and P.J. Pigram. 2011. Carboxylic acids affect sorption and micro-scale distribution of phosphorus in an acidic soil. Soil Sci. Soc. Am. J. 75:35-44.

Shober, A.L., D.L. Hesterberg, J.T. Sims, and S. Gardner. 2006. Characterization of phosphorus species in biosolids and manures using XANES spectroscopy. J. Environ. Qual. 35:1983-1993.

Seiter, J.M., K. E. Staats-Borda, M. Ginder-Vogel, and D.L. Sparks. 2008. XANES spectroscopic analysis of phosphorus speciation in alum-amended poultry litter. J. Environ. Qual. 37:477-485.

Tejedor-Tejedor, M.I., and M.A. Anderson. 1990. Protonation of phosphate on the surface of goethite as studied by CIR-FTIR and electrophoretic mobility. Langmuir. 6:602-611.

Toor, G.S., S. Hunger, J.D. Peak, J.T. Sims, and D.L. Sparks. 2006. Advances in the characterization of phosphorous in organic wastes: Environmental and agronomic applications. *In* Advances in Agronomy (ed: D.L. Sparks), Vol. 89:1-72. Elsevier, San Diego, CA.

Violante, A., and M. Pigna. 2002. Competitve sorption of arsenate and phosphate on different clay minerals and soils. Soil Sci. Soc. Am. J. 66:1788-1796.

Webb, S.M. 2005. SIXpack: A graphical user interface for XAS analysis using IFEFFIT. Physica Scripta. T115:1011-1014.

Yang, J., M.O. Bennett, P.M. Jardine, N.T. Basta, and S.W. Casteel. 2002. Adsorption, sequestration, and bioaccessibility of As(V) in soils. Environ. Sci. Technol. 36:4562-4569.

Yu, W.H., C.M. Harvey, and C.F. Harvey. 2003. Arsenic in groundwater by arsenic in Bangladesh: A public health emergency. Bull. World Health Organ. 39.

Chapter 2

SOIL PHOSPHORUS SPECIATION USING MICROSPECTROSCOPIC TECHNIQUES

2.1   Introduction

Phosphorus (P) is an essential nutrient for plant growth and is widely-applied to agricultural soils in fertilizers and manures. Frequent application of P fertilizer often leads to excessive soil test P ratings based on agronomic soil tests. Soil P is sometimes vulnerable to loss to surface and groundwater sources through runoff and leaching processes. High P concentrations in surface water supplies can cause eutrophication and adversely affect water quality. It is important to understand the species (forms) of P present in soils to determine the best methods to prevent P loss from erosion, runoff, and leaching.

Traditional methods for soil P speciation often rely on chemical extractions, which identify operationally-defined P species and can introduce artifacts during analysis. Spectroscopic techniques, such as Fourier Transform Infrared Spectroscopy (FTIR) and Nuclear Magnetic Resonance (NMR) spectroscopy, have been used to characterize P species in pure mineral systems or soil extracts, but are not sensitive enough to speciate P in soils due to spectral interference from other soil components (Piersynski et al., 1990; Cade-Menun and Liu, 2013). Traditional techniques to measure crystalline minerals in soil, such as X-ray diffraction, are limited by the low concentration of soil P minerals relative to other mineral components (Piersynski et al., 1990). X-ray absorption spectroscopy (XAS) is a non-invasive spectroscopic technique that can overcome several limitations of indirect methods to speciate soil P.

25

Phosphorus K-edge X-ray absorption near edge structure (XANES) has been used previously to characterize the chemical forms of P in bulk samples, including soils (Beauchemin et al., 2003; Sato et al., 2005) poultry litter (Peak et al., 2002; Sato et al., 2005; Shober et al., 2006), and other manures and biosolids (Shober et al., 2006) for bulk samples. XANES spectra exhibit distinct characteristics based on the chemical environment of P in a sample. For example, XANES spectra for calcium (Ca) phosphate minerals have a characteristic post-edge shoulder from approximately 2 to 6 eV above the P K-edge (Hesterberg et al., 1999) and spectra for phosphate bound to oxidized iron [Fe(III)] have a pre-edge feature approximately -2 to -4 eV relative to the P K-edge white line (Khare et al., 2004). Aluminum (Al) phosphate minerals can be distinguished based on secondary peak positions (Ingall et al., 2011). Linear combination fitting (LCF) can be used to estimate the composition of P species based on bulk XANES spectra but is not able to account for all possible P species in a soil or manure sample. Therefore, it can be difficult to precisely interpret bulk XANES results for soils.

A higher degree of certainty for P speciation can be achieved by focusing the X-ray beam to a size similar to soil particles. To achieve spatially-resolved P speciation, micro X-ray fluorescence (μ-XRF) can be used to map the distribution of elements of interest for P speciation (i.e., Al, Fe, Ca, and Si). Following μ-XRF analysis, micro-focused XANES (μ-XANES) spectra can be used to examine the bonding environment of P. A handful of scientists have used μ-XRF analysis of P, Al , and Si in combination with μ-XANES to examine P speciation in environmental samples such as marine sediments (Brandes et al., 2007; Giguet-Covex et al., 2013) and speleothems (Frisia et al., 2012;), but these techniques have not been widely applied to soils. Lombi et al. (2006) and Schefe et al. (2011) used spatially-resolved XANES studies to compare the effectiveness of fertilizers applied to soils in laboratory settings at high concentrations.

26

Advancements in synchrotron capabilities, such as increased stability of X-ray sources, and improved beamline optics, will allow for better characterization of P at the molecular level. This study examines the capabilities and limitations of μ-XRF and μ-XANES to speciate P in heterogeneous soil samples to increase the fundamental understanding of P chemistry in agricultural soils. To our knowledge, this is the first study to examine P speciation with μ-XANES *in situ* for soil samples. Furthermore, this is the first study to compare μ-XRF maps from a tender energy imaging beamline (1-5 keV) and a high-energy (4.5-24 keV) imaging beamline to assess the elemental distribution of P with Fe and Ca.

2.2   Materials and Methods

2.2.1   Soil Collection and Characterization

Soils from four agricultural fields within the Mid-Atlantic region with high (>900 mg kg^{-1}) total P loadings were selected to evaluate soil P speciation. Soils included a Davidson silty clay, Hagerstown silty clay loam, Berks silt loam, and Mullica-Berryland sandy loam. Samples were collected from the top 5 cm of soil. A more detailed description of Davidson, Hagerstown, and Berks soil samples can be found in Shober and Sims (2007). The Mullica-Berryland soil is currently managed under grain production and historically received high applications of broiler litter.

Prior to analysis, soil samples were air-dried, ground, and sieved to <2 mm particle size. Characterization of pH, organic matter content, particle-size, Mehlich3-extractable elemental content were performed according to standard methods at the University of Delaware Soil Testing Laboratory (Northeast Coordinating Committee,

2011). EPA microwave-assisted acid digestion method 3051b was used for total P, Fe, Al, and Ca analyses (EPA, 1995). An ammonium oxalate extraction was completed according to procedures in Jackson et al. (1986) to estimate amorphous Al- and Fe- oxide content. Prior to ammonium-oxalate extractions, soluble salts and organic matter were removed according to methods in Kunze and Dixon (1986). Soils were ground to a fine powder, and 0.25 g of soil was weighed into a 50-mL centrifuge tube covered in Al foil. Fifty mL of 0.2 M ammonium-oxalate was added, and the reaction was shaken for 2 h. Extractions were filtered to 0.2 μm and measured with inductively coupled plasma-atomic emission spectroscopy for Fe and Al content.

X-ray diffraction (XRD) analysis was completed at the XRD1 beamline at the Brazilian Synchrotron Light Laboratory (LNLS) to characterize the soil mineralogy. Pretreatment of soils to remove soluble salts, organic matter, and Fe oxides was carried out according to methods in Kunze and Dixon (1986) prior to XRD analysis. Samples were divided into sand, silt, and clay fractions. For the Davidson soil, the clay fraction was divided into coarse- and fine- clay fractions for XRD analysis due to the high clay content. Clay fractions were pretreated according to methods in Whittig and Allardice (1986) and loaded into quartz capillary tubing for analysis at the XRD1 beamline.

2.2.2 Micro-XRF and Micro-XANES Analysis

Soil samples were loaded into EPO-TEK® epoxy resin, thin-sectioned to 30 μm at Spectrum Petrographics, and mounted to a quartz slide. This mounting technique was used for μ-XRF and μ-XANES experiments to provide optimal P detection and allow samples to be run at multiple beamlines. Tender-energy (1-5 keV) X-ray beamlines X15B at the National Synchrotron Light Source (NSLS) and 14-3 at the Stanford Synchrotron

Radiation Lightsource (SSRL) were used for μ-XRF mapping of P, Al, and Si distribution and μ-XANES analysis at the P K-edge. Tender-energy XRF maps at beamline X15B were collected at 2525 eV with a 20-μm step-size and 2-s dwell time. At 14-3, XRF maps at 2240 eV were collected with 10-μm step-size and 50-ms dwell time. Kirkpatrick-Baez mirrors were used at both beamlines to focus the beam to micron scale. The sample stage and detector at beamlines X15B and 14-3 were kept under a He atmosphere during the experiments to reduce backscatter. Beamline 2-3 at SSRL was used for XRF mapping of Si, Fe, and Ca distribution. Maps at beamline 2-3 were collected at 12,000 eV with 5-μm step size and 20-ms dwell time. The storage ring at SSRL was operated at 3 GeV with a ring current of approximately 500 mA.

Phosphorus hotspots identified in μ-XRF maps were examined further with μ-XANES analysis. XANES spectra were collected in fluorescence mode since only the top few microns of sample are penetrated at the low energy required for P K-edge excitation. Samples were oriented at 45° to the incident beam and a PIPS (Passivated Implanted Planar Silicon) detector was positioned at 90° to the incident beam. Spectra were collected over 2100 to 2140 eV with a 2-eV step-size, 2140 to 2160 eV with a 0.2-eV step-size, and 2160-2200 eV with a 0.5-eV step-size. At beamline X15B, approximately 20 XANES scans per hotspot were averaged to increase spectral quality. At beamline 14-3, two to four scans per hotspot were averaged. To ensure spectral reproducibility, the position of the white line was measured for repeated scans and did not vary by more than ±0.1 eV for repeated scans of assessed hotspots.

2.2.3 Standards

Spectra for phosphate mineral standards from Ingall et al. (2011) were used for comparison to samples in this study, and XANES were collected in fluorescence mode at beamline X15B at the NSLS. Further details regarding P K-edge XANES spectra collection for mineral standards can be found in Ingall et al., (2011). Spectra for organic and sorbed P standards were collected at the LNLS tender-energy beamline SXS in fluorescence mode. The monochromator used for these measurements was equipped with a double-crystal InSb (111) and the electron storage ring was operated at 1.37 GeV with a current range of about 110 to 250 mA.

2.2.4 Data Processing

Sam's MicroAnalysis Toolkit (Webb, 2005) was used to process XRF maps and create tri-color images of P, Al, and Si for maps collected at 2240 eV and Fe, Ca, and Si for maps collected at 12,000 eV. Fluorescence for each element was normalized to the highest concentration; areas with the highest fluorescence counts are represented with brightest colors in tri-color maps. Corresponding areas from 14-3 and 2-3 XRF maps were identified by visually comparing Si maps from each beamline. Raw XANES spectra were averaged using Sixpack software (Webb, 2005). Background subtraction and pre- and post-edge background corrections were performed in Athena (Ravel and Newville, 2005). The center of the primary peak in the XANES spectra was chosen as E_0; this method is preferred for P K-edge analysis since pre-edge features may affect the edge position of spectra. Distinct pre-and post-edge features apparent in P K-edge XANES spectra for points of interest (POIs) in soils were compared to spectra of known standards (Fig. 1.1) to examine P speciation, a technique referred to as "fingerprinting."

It is difficult to avoid some degree of self-absorption at the low energy at which P K-edge XANES spectra are collected, particularly in spatially-resolved XANES (Lombi et al., 2006; Schefe et al., 2010). Although self-absorption affects the amplitude of signals in XANES spectra, it does not affect the location of features within the spectra. Therefore, spectral features are discussed based on peak positions and separation of peak features rather than amplitude in this study.

2.3   Results and Discussion

2.3.1   Soil Characterization

Soil chemical and physical properties are reported in Table 2.1 and 2.2. Soils in this study demonstrated a range of chemical and physical properties, such as pH, texture, and amorphous Fe and Al-oxide content. Soil pH ranged from 4.2 to 6.4, a range that would be expected for Mid-Atlantic soils. Organic matter content was consistent between soil types, ranging from 33-38 mg kg^{-1} soil. Total P concentrations ranged from 985-1256 mg kg^{-1} soil. The Mullica-Berryland soil was the most coarse-textured of soils evaluated, but also contained the highest total P and Mehlich3-extractable P content. Arai and Livi (2013) provide evidence that up to 50% of P in heavily-fertilized agricultural soils from southern Delaware may be present in the sand fraction. The high plant-available P, as represented by Mehlich3-extractable P, in the Mullica-Berryland soil is expected due to its low ammonium-oxalate extractable Fe and Al content. Concentration of Fe and Al oxide content is important to this study due to the high affinity of these soil components to retain P. Total Fe and Al content was highest for the Davidson soil, which also contains the highest percentage of clay. The Davidson soil has

31

the lowest Mehlich3-extractable P content. It is not surprising that the Davison soil has the lowest plant-available P, since Fe- and Al-oxides are known to have a high sorption capacity for P at low pH (Bleam et al., 1991; Arai and Sparks, 2001). Hagerstown and Berks soils are have similar pH and total Fe and Al contents, with the Hagerstown having lower sand content and higher ammonium-oxalate extractable Al and Fe.

2.3.2 Micro-XRF and XANES Analysis

2.3.2.1 Standards

Features for XANES spectra collected from P points of interest (POIs) in soils were compared to XANES spectra for known standards. Distinct pre- and post-edge features apparent in P K-edge XANES spectra were used to assess P speciation by "fingerprinting." Peak positions for the center of the primary fluorescence peak and other spectral features can be observed in Table 2.3. The primary fluorescence peak was centered at 2154.4 to 2151.6 eV for Ca-phosphate standards and 2151.9 to 2152.1 eV for Fe- and Al-associated P species (Table 2.3). All P analyzed was in the P(V) oxidation state based on the position of the primary fluorescence peak. A pre-edge feature is observed at approximately 2148.5 eV for all standards associated with oxidized Fe and is more defined for Fe phosphate mineral phases than sorbed phosphate species due to the increased number of P atoms bound to oxidized Fe. This distinction has been observed in numerous previous studies (Hesterberg et al., 1999; Khare et al., 2004; Shober et al., 2006; Brandes et al., 2007). A post-edge shoulder was observed at approximately 2154.1 eV for Ca phosphate mineral species. The center of the primary

fluorescence peak for the organic phospholipid standard was located at 2151.6 eV, and a secondary peak was located at approximately 2166.8 eV

2.3.2.2   Mullica-Berryland Soil

Initial spectra collected at the NSLS X15B beamline indicated the presence of Al- and Ca-bound phosphorus in soils with high concentrations of total P (Fig. 2.1). The association of Al and P from XRF map is seen in Fig 2.2b. Based on the lack of spectral features and co-location with Al in XANES spectra for this point, it is hypothesized this phosphate is sorbed to an Al-oxide (Fig 2.2c). Other spectra (Fig. 2.2d) indicate the presence of an apatite-like mineral based on the post-edge shoulder observed at approximately 2154 eV and the secondary peaks at 2162 and 2169 eV. Apatite is a commonly-observed mineral in soil, and XANES analysis has been used to demonstrate that apatite can occur in soils through natural weathering processes (Giguex-Covex et al., 2013) or from P fertilizer application (Kar et al., 2012).

A more detailed speciation analysis of the Mullica-Berryland soil was completed at SSRL beamline 14-3. Micro-XRF maps in Fig. 2.3 and 2.4 demonstrated the elemental distribution of P, Al, Si, Fe, and Ca. It should be noted that the approximate sampling depth for P fluorescence in soil ranges from 2-10 μm, while fluorescence for Ca and Fe likely penetrated the entire 30-μm thickness of the sample. Therefore, inferences regarding co-location of P with Ca or Fe should be verified based on features observed in μ-XANES spectra.

Phosphorus is distributed heterogeneously throughout the soil sample, with some P hotspots containing highly-concentrated regions of P and others containing more diffuse P regions. Phosphorous speciation is often easier to discern in P-rich

particles (Piersynski et al., 1990). The Mullica-Berryland soil contains over 75% sand, and XRF maps confirm high sand content based on the large number of Si-rich particles larger than 50 μm in diameter. Based on the distribution of Fe and Al in XRF maps (Fig 2.3 and 2.4), it can be assumed that metal oxide coatings are present on several sand particles.

Co-location of P and Ca is evident for several Mullica-Berryland POIs (i.e., 1, 2, 3, 4, 5, 8, and 9) through visual inspection of XRF maps in Fig. 2.3 and 2.4. Direct correlation analysis for P and Ca was not possible since fluorescence was collected at different beamlines for the two elements, but the association of P with Ca is confirmed by the presence of a post-edge shoulder at 2154 eV and a slight downward shift of approximately 0.4 eV for the primary fluorescence peak in XANES spectra for each of these POIs. Calcium and P is concentrated in localized regions at all POIs except 4, in which P and Ca are diffusely distributed and appear to be dispersed in a metal-oxide coating around a sand particle. Less self-absorption affects POI 4 compared to POIs 1, 2, and 3 based on the increased peak height for the white line, likely because P is more diffuse in this region. Secondary features are observed at approximately 2161.7 and 2168.3 eV for POIs 1, 2, 3, and 4, which are similar to the spectral features of apatite. Small variations in secondary peak configuration may be caused by substitutions of Fe and Mn into the apatite structure, since the strength of the post-edge shoulder is related to the number of Ca atoms to which P is bonded (Ingall et al., 2011). A low signal-to-noise ratio prevents definitive identification of secondary peaks in POI 5 and 8, but intensity of the post-edge shoulder suggests that these P hotspots are an apatite-like Ca species. The post-edge shoulder is less distinct in the spectra for POI 9 and may represent a less-crystalline apatite or monetite species. Spectra for monetite and non-

crystalline apatite are very similar, and difficulty in differentiating these spectra has been previously observed (Ingall et al., 2011).

For POI 7 in the Mullica-Berryland soil, a pre-edge feature at 2148.5 eV and a broad secondary peak at 2168 eV demonstrate that this is likely P sorbed to an amorphous Fe oxide material. This is confirmed by co-location of P with Fe in XRF maps. The XANES spectrum for POI 10 also contains a pre-edge feature, and secondary peaks for this hotspot show slightly more detail; a small peak at 2158 eV indicates that P is sorbed to a more crystalline Fe oxide mineral and is similar to the peak observed in phosphate sorbed to goethite (Fig 2.1). Monnier et al., (2011) also observed a small peak approximately 7 eV above the white line has for phosphate sorbed to goethite, with the intensity of the peak increasing as crystallinity of goethite increased.

Point of interest 6 and POI 11 contain few distinct features to clearly identify P speciation in these hotspots. However, POI 6 does show some correlation with manganese (Mn) (data not shown) and could suggest a sorbed P species to Mn-oxide. POI 11 shows correlation of P with Al and Fe and is incorporated in a metal-oxide coating on a Si-rich particle. Since a pre-edge feature is clearly not observed in the spectra, this is likely an Al oxide-sorbed P species. Using scanning transmission electron spectroscopy paired energy-dispersive X-ray analysis, Arai and Livi (2013) also observed that P can be associated with mixed amorphous Fe- and Al-oxide coatings on sand particles.

The Mullica-Berryland soil has a high sand content and a long history of poultry litter application. This soil contains a low concentration of Fe- and Al-oxides compared to other soils examined in this study; Fe- and Al-oxides are known to strongly adsorb P via inner-sphere complexation (Tejedor-Tejedor and Anderson, 1986; Luengo et al., 2006; Del Nero et al., 2010; Li et al., 2013). Calcium phosphate minerals were the

primary P species identified in the Mullica-Berryland soil. Calcium phosphates were probably contributed from manure additions to the soil. Sharpley et al. (2004) observed increases in the contribution of Ca-associated P compared to Fe- and Al-associated P in soils that had been amended with poultry manure for >10 years. A variety of metal oxide-sorbed species were also observed in the Mullica-Berryland soil. Beauchemin et al. (2003) also observed that Ca phosphate minerals, Fe-oxide sorbed, and Al-oxide sorbed phosphates were the predominant P form in agricultural soils with high total P concentration (>800 mg kg^{-1}) at low pH ($\leq$ 6.2).

2.3.2.3   Davidson Soil

The Davidson soil is fine-textured and classified as a silty clay. It contains the highest Fe (11.2%) and Al (6.1%) contents of the soils investigated in this study. X-ray fluorescence maps show a high distribution of Fe and Al throughout the soil (Fig. 2.5). There is a much lower distribution of Si and Ca throughout the sample compared to the XRF maps for the Mullica-Berryland soil. Low Si content was expected due to the low sand content ($\sim$2%) in this soil. Approximately 2% of total P for the Davidson was extracted with Mehlich3, indicating that the majority P is strongly-retained in soils. Fluorescence maps demonstrates that P is present in both diffuse and concentrated regions within soil aggregates.

Co-location of P with Ca is observed in XRF maps for the Davidson soil for POI 1 (Fig 2.5). The XANES spectrum for this POI contains a post-edge shoulder at approximately 2154.5 eV and secondary peaks observed at 2161 and 2168.5 eV, consistent with XANES features for apatite. The weakness of the post-edge shoulder could indicate a less-crystalline form of apatite. At POIs 2 through 6 in the Davidson

36

soils, XRF maps show co-location of P with Fe, although Fe fluorescence is diffuse in these locations. A definitive pre-edge feature is observed at approximately 2148.8 eV in each XANES spectra, confirming that P is associated with oxidized Fe. The secondary peak features are similar for POI 2 through 6, showing a broad peak at approximately 2168 eV. It can be assumed that these hotspots contain some P sorbed to amorphous Fe oxide material. Phosphorous appears in many of these POIs as P-rich particles within a soil aggregate. Co-location of P with Al is also apparent in POIs 2 through 6, and it is possible that amorphous Al oxide-sorbed P could contribute to the XANES spectra. This cannot be confirmed with linear combination fitting due to the apparent self-absorption observed in XANES spectra for many POIs. For POI 7, a broad, secondary peak is present in the same location as other Fe-associated hotspots, but signal-to-noise ratio is too low to clearly identify speciation.

A large percentage of hotspots in the Davidson soil contained P sorbed to Fe oxide minerals; this is not surprising due to the high total and ammonium-oxalate extractable Fe and Al concentrations in the Davidson soil. Points of interest 3, 4, and 5 exhibit the highest degree of self-absorption, but are also the least noisy of the spectra. Compared to many spectra for other soil samples, XANES spectra for the Davidson soil have an overall lower degree of self-absorption because P is more diffusely distributed throughout the soil.

2.3.2.4   Hagerstown Soil

The XRF maps for the Hagerstown soil demonstrate that Si, Fe, and Al are correlated in many soil particles, indicating a large proportion of aluminosilicate particles with some degree of Fe substitutions are present (Fig. 2.6). Soil aggregates

containing various-sized particles with high concentrations of Si, Fe, Ca, or Al are also observed. Several concentrated regions with high Ca fluorescence are present in this soil. Co-location of P and Ca hotpots is observed in POI 1. The XANES spectra for this POI shows a post-edge shoulder at 2154.3 eV and secondary peaks at 2162 and 2169 eV, consistent with peak locations for apatite. For POI 2, a highly concentrated P hotspot is observed in XRF maps, but this region was not mapped in the higher-energy XRF map. The same post-edge shoulder and secondary peaks are observed in spectra for POI 2, indicating the presence of apatite. The primary fluorescence peaks for POI 1 and 2 are shifted approximately –0.4 eV compared to the white line for POI 3, 4, and 5; this shift is consistent with those observed in Lombi et al. (2006) for Ca phosphate minerals compared to Fe and Al-bound P species. We assume that both POI 1 and 2 are crystalline forms of apatite based on their distinct secondary peak features. Crystalline minerals exhibit strong orientation-dependence in the EXAFS region of the spectra (Manceau et al., 2000); POIs 1 and 2 show differences in spectra above 2180 eV providing evidence that apatite is crystalline and was sampled at different orientations.

Spectra for POI 4 and 5 contain distinct pre-edge features at 2148.5 eV, indicating the presence of oxidized Fe species. Co-location of P with Fe is apparent for POIs 3, 4, and 5, and secondary features of XANES for these hotspots are most related to those of strengite. However, for POI 3, the pre-edge feature is dampened. Substitutions of other transition metals, such as Fe(II) or Mn(II), into the crystal lattice commonly occur in soil minerals and can result in weakened pre-edge features. Structure above 2180 eV does not change significantly in spectra for POI 3, 4, and 5. Strengite in these regions appears to be in a less-crystalline form, since structural changes in the lower EXAFS region of the spectra would likely appear if strengite were crystalline. Based on XRF maps, the Fe-associated phosphate at POI 4 appears to be contained within a larger

soil aggregate containing Si, Al, and Fe, and the Fe phosphate mineral in POI 5 appears to be part of an Fe coating on a sand particle.

The Hagerstown soil contained both Fe and Ca phosphate mineral species. Spectra for Ca phosphate species show more self-absorption than Fe phosphate species based on the dampened amplitude of the primary fluorescence peak. Despite a high amorphous Fe- and Al-oxide concentration, as indicated in ammonium-oxalate extractions, sorbed species of P were not detected in the Hagerstown soil. Although sorbed P species likely exist in the Hagerstown soil, regions containing adsorbed P may have been too diffuse to obtain quality XANES spectra. This sample has a lower total P concentration than the Mullica-Berryland and Davidson soils, which may have contributed to the difficulty in obtaining quality XANES spectra for this soil.

2.3.2.5   Berks Soil

The Berks soil contains over 60% silt and 141 mg kg^{-1} Mehlich3-extractable P. This soil also contains 1259 and 879 mg kg^{-1} ammonium-oxalate extractable Fe and Al, respectively. Unique P features are observed in the XRF maps for the Berks soil (Fig. 2.7). For example, in the region containing POI 3, P is correlated with Ca and appears to be a coating on a soil particle. However, no Si, Al, or Fe is present in this region. In the P region containing POI 2, a streak of P and Ca can be seen within a soil aggregate. Except in these two locations, P appears in discrete, P-rich particles throughout the Berks sample.

Phosphorus appears to be co-located with Fe in POI 1 based on XRF maps, but the XANES spectra does not contain a pre-edge feature as would be expected for P associated with oxidized Fe. Instead, a post-edge shoulder is observed at approximately

39

2154 eV, most likely indicative of a Ca phosphate species. Although a slight post-edge shoulder can indicate XANES spectra for potassium phosphate (Brandes et al., 2007; Rouff et al., 2009), it is unlikely that a potassium phosphate mineral is present in this soil. The shoulder of POI 1 is very distinct and self-absorption is low compared to XANES spectra for other Ca phosphates observed in this study. Although Ca fluorescence is low for this P hotspot, the low concentration of Ca phosphate likely decreases self-absorption. In POI 2, correlation of P and Ca are clearly observed in XRF maps, and spectral features align with an apatite-like Ca phosphate mineral.

Phosphorus and Ca are also co-located in POI 3 according to XRF maps, but a post-edge shoulder is not present in the XANES spectra. This spectrum has a low signal-to-noise ratio and speciation is for POI 3 is unclear. The peak height of the primary fluorescence peak in POIs 4, 5, 6, and 7 is severely reduced, apparently due to self-absorption. Self-absorption typically affects spectra to differing degrees, based on the local concentration of P. For example, Hagerstown POIs 1 and 2 appear to be the same Ca phosphate mineral but primary fluorescence peak heights are not equally reduced. However, the spectra in Berks POIs 4, 5, 6, and 7 are nearly identical in peak height and features, indicating that maximum self-absorption has occurred. Maximum self-absorption is a possibility since the approximate sampling depth for P fluorescence in most soil minerals ranges from 2 to 10 µm. The center of the primary fluorescence peak for POIs 3 through 7 is aligned with the position for Ca phosphate minerals or organic P species. However, no other features were discerned in these spectra, and more exact speciation information cannot be confirmed.

2.4 Conclusions

Initial data from µ-XRF and µ-XANES analyses indicate the presence of Ca phosphates, Fe(III) phosphates, Al-sorbed phosphate, and Fe-sorbed phosphate in low pH agricultural soils from the Mid-Atlantic. Calcium phosphates were distinguished from other species by a slight downward shift in the position of the primary fluorescence peak and the presence of a post-edge shoulder, and the presence of a pre-edge feature was key in determining the presence of oxidized Fe associated with P. X-ray fluorescence maps were useful for distinguishing Al-oxide sorbed P from Fe-oxide sorbed P. A low signal-to-noise ratio often limited data collection in regions with diffuse, low-concentrations of P, and quality XANES spectra were more easily obtained for discrete, P-rich particles. Therefore, some forms of P, such as organic P species, were likely not detected during analysis. Difficulty in distinguishing organic P species may have resulted because P concentration was too low for detection in regions containing organic P. Radiation damage has also been shown to affect the collection of XANES for organic P species (Brandes et al., 2007).

This study emphasizes the importance of pairing analyses of tender-energy and high-energy XRF maps to aid with P speciation. To our knowledge, previous µ-XANES studies have not used this technique and, therefore, have not been able to evaluate co-location of P with Fe or Ca. Micro-XANES analysis offers advantages for speciation of inorganic P compared to IR and NMR techniques, as soils can be measured *in situ*. Even with varying degrees of self-absorption and signal-to-noise ratios in µ-XANES spectra, important inferences regarding P speciation can be made. With future advances in XAS technology, it is expected that µ-XANES spectral resolution at the P K-edge will improve. This study highlights the potential of µ-XANES analysis for use in environmental and

agricultural sciences. A variety of studies can benefit from paired μ-XRF and μ-XANES

analysis, such as studies to evaluate changes in P speciation after fertilization or during P

transport.

Table 2.1. Characterization analysis of pH, organic matter (OM), particle-size fractions, ammonium-oxalate extractable Al (Al_{ox}), ammonium-oxalate extractable Fe (Fe_{ox}), and total phosphrous (P), iron (Fe), aluminum (Al), and calcium (Ca) concentrations for Mullica-Berryland, Davidson, Hagerstown, and Berks soils.

Soil Series	pH	OM	Sand	Silt	Clay	Al_{ox}	Fe_{ox}	Total P	Total Fe	Total Al	Total Ca
		— g kg^{-1} —	———%———			——— mg kg^{-1} ———			——— g kg^{-1} ———		
Mullica-Berryland	4.2	38	78.4	8.2	13.4	549	507	1256	1.6	6.3	0.96
Davidson	6.4	31	2.3	50.4	47.3	1284	1390	1216	112.2	60.9	1.22
Hagerstown	5.6	36	1.5	62.9	35.6	1146	1453	986	25.9	20.5	2.04
Berks	5.5	36	14.7	58.9	26.4	879	1259	985	29.8	21.2	1.98

Table 2.2. Mehlich-3 extractable phosphorus (P), potassium (K), calcium (Ca), magnesium (Mg), manganese (Mn), zinc (Zn), copper (Cu), iron (Fe), boron (B), sulfur (S), and aluminum (Al) for Mullica-Berryland, Davidson, Hagerstown, and Berks soils.

Soil	Mehlich3-Extractable Elements										
	P	K	Ca	Mg	Mn	Zn	Cu	Fe	B	S	Al
	mg kg^{-1}										
Mullica-Berryland	668.3	133.7	852.2	61.2	21.4	27.3	12.5	140.0	0.2	33.3	1449.5
Davidson	27.4	82.2	972.5	329.1	217.3	9.1	11.7	65.7	1.3	19.8	987.9
Hagerstown	111.9	299.3	1472.9	176.5	203.3	4.3	1.9	147.8	1.1	32.7	938.0
Berks	141.0	256.8	1319.5	169.4	249.7	9.1	4.1	170.9	1.3	24.8	775.7

Table 2.3. Energy (eV) positions for features observed XANES spectra for mineral,

sorbed, and organic standards, and points of interest (POIs) in soil samples.

Standard	Center	Pre-edge	Post-edge	Secondary peaks		
Fluorapatite	2151.4	–	2154.2	2162	2168.6	
Monetite	2151.5	–	2154	2162	2167.6	
Poorly-crystalline Apatite	2151.6	–	2154.2	2162	2167.8	
Strengite	2152	2148.5	–	2157.2	2161.8	2168.4
PO_4 sorbed to goethite	2151.9	2148.5	–	2158.3	2168.3	
PO_4 sorbed to ferrihydrite	2151.9	2148.5	–	2168.2		
Variscite	2152.1	–	–	2158.5	2169	
PO_4 sorbed to Al hydroxide	2152	–	–	2157.5	2168.7	
Phospholipid	2151.6	–	–	2166.8		

Soil	POI	Center	Pre-edge	Post-edge	Secondary peaks		
Mullica-Berryland	1	2151.3	–	2154	2161.7	2168.1	
	2	2151.4	–	2154	2161.9	2168.5	
	3	2151.6	–	2154	2161.6	2168.4	
	4	2151.6	–	2154.2	2161.5	2168	
	5	2151.5	–	2154		not definitive	
	6	2151.7	–	–		2168.9	
	7	2151.8	2148.5	–		2168.2	
	8	2151.6	–	2154	2161.5	2167.4	
	9	2151.6	–	2154	2161.6	2167.5	
	10	2151.9	2148.5	–		2167.5	
	11	2151.8	–	–		2167	
Davidson	1	2151.6	–	2154.5	2161.03	2168.6	
	2	2152	2148.8	–		2168	
	3	2152	2148.8	–		2168	
	4	2152	2148.8	–		2168	
	5	2152.1	2148.8	–		2168	
	6	2152	2148.8	–		2168	
	7	2152.2	–	–		2168	
Hagerstown	1	2151.4	–	2154.3	2162.1	2168.7	
	2	2151.5	–	2154.3	2161.6	2168.3	
	3	2151.8	–	–	2157.1	2164.7	2168.9
	4	2151.8	2148.5	–	2158.1	2161.6	2168.1
	5	2151.9	2148.4	–	2158.9	2163.4	2168
Berks	1	2151.4	–	2154	2161.9	2168	
	2	2151.4	–	2154	2162	2169	
	3	2151.6	–	–		2168	
	4	2151.6	–	–		2168	
	5	2151.6	–	–		2168.5	
	6	2151.6	–	–		2168.5	
	7	2151.6	–	–		2168.1	

Figure 2.1. XANES spectra for various Ca phosphate mineral (pink), Fe-associated (blue), Al-associated (green), and organic P species (teal).
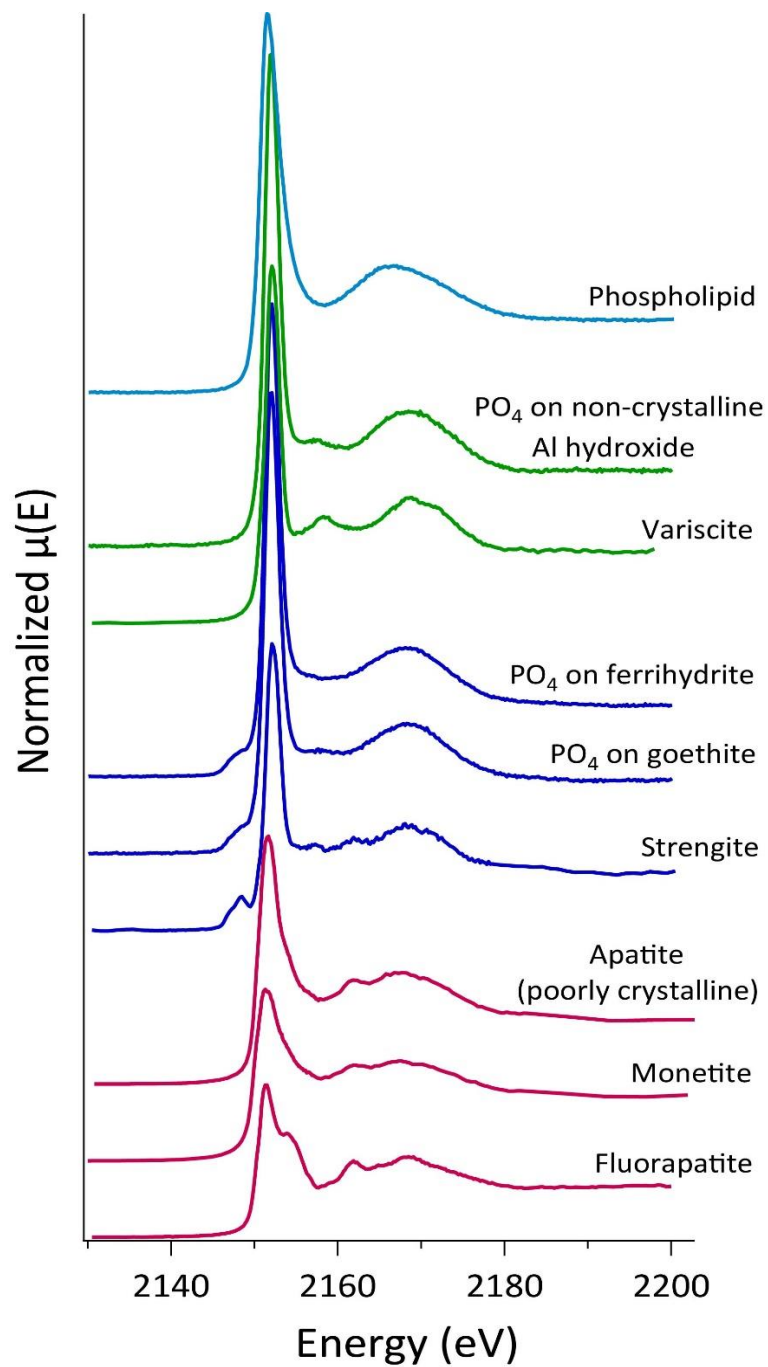
Figure 2.2. NSLS X15B data showing a 1.5 × 1.5 mm XRF P map (a) and 100 × 100 μm P and Al XRF maps (b) of the Mullica-Berryland soil. Correlation of P and Al is observed. P K-edge XANES spectra confirm presence of Al-associated PO4 (c) and apatite (d) (corresponding XRF map not shown for d).
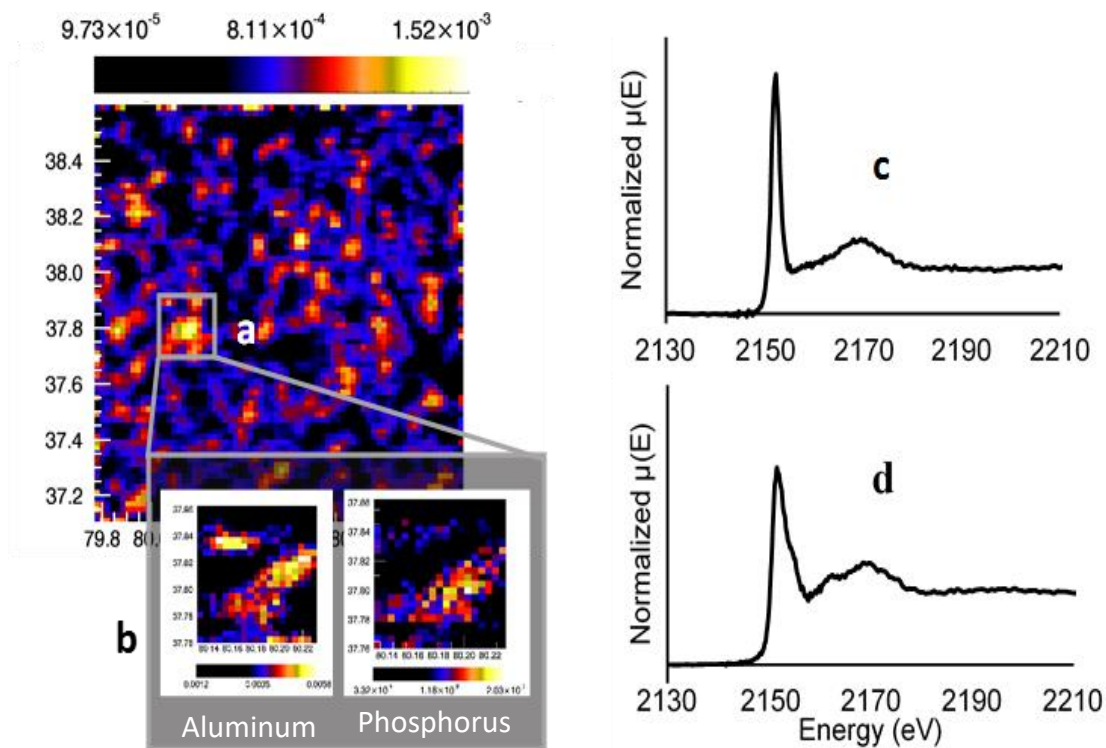
Figure 2.3. Tender-energy X-ray fluorescence maps showing the elemental distribution of P (red), Al (green), and Si (blue) and corresponding P K-edge XANES spectra collected at SSRL beamline 14-3 for the Mullica-Berryland soil.
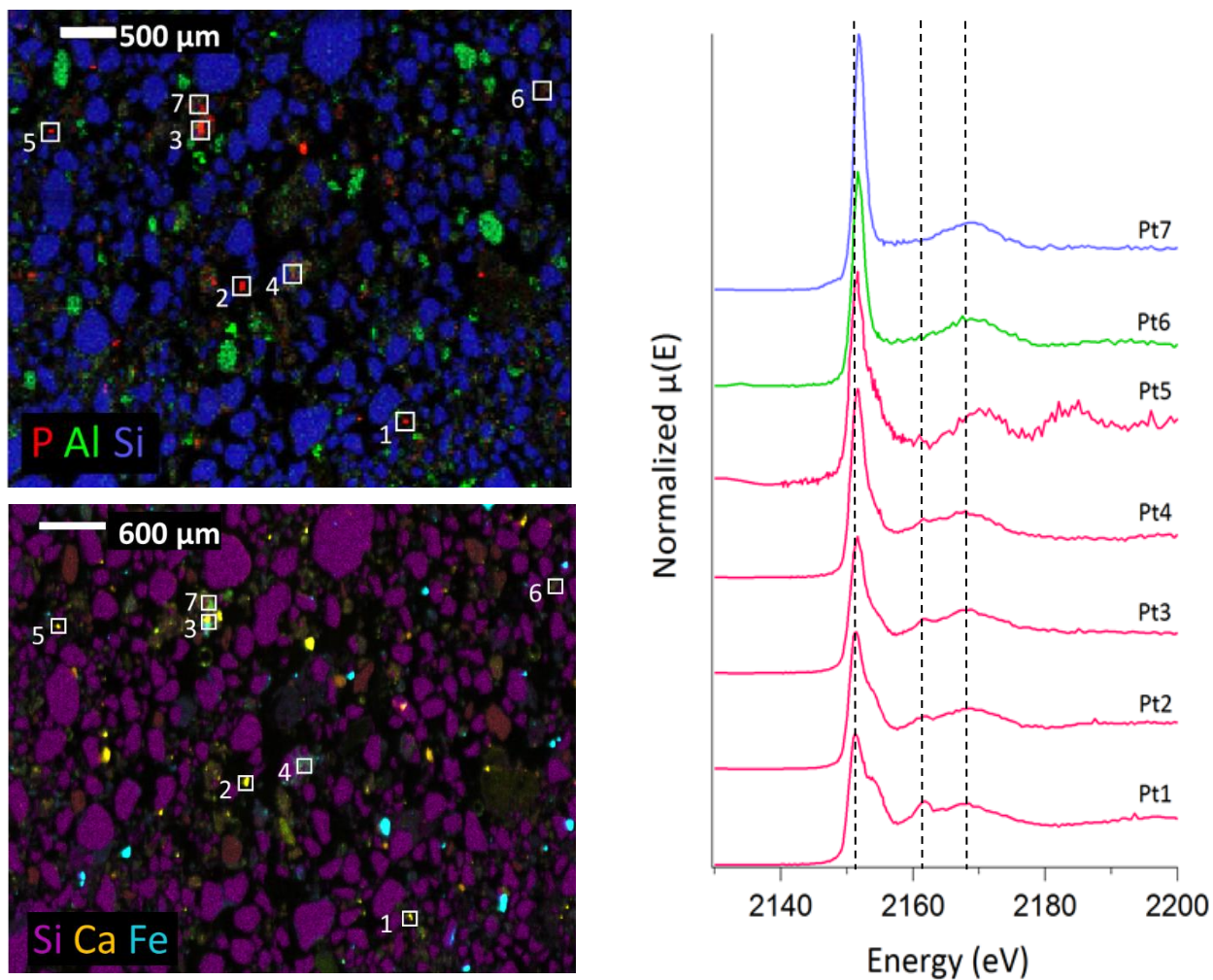
Figure 2.4. Tender-energy X-ray fluorescence maps showing the elemental distribution of P (red), Al (green), and Si (blue) and corresponding P K-edge XANES spectra collected at SSRL beamline 14-3 for the Mullica-Berryland soil.
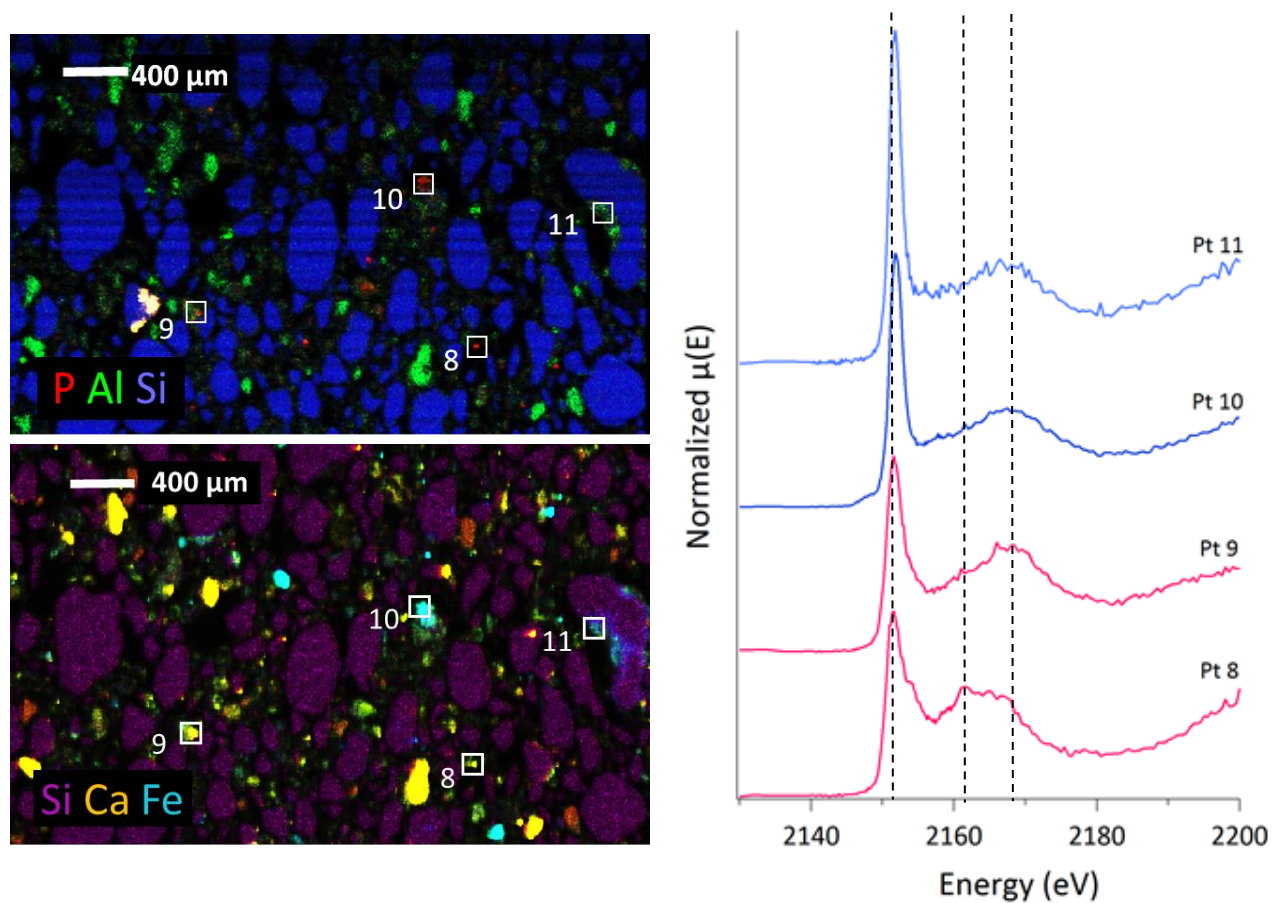
Figure 2.5. Tender-energy X-ray fluorescence maps showing the elemental distribution of P (red), Al (green), and Si (blue) and corresponding P K-edge XANES spectra collected at SSRL beamline 14-3 for the Davidson soil.

Figure 2.6. Tender-energy X-ray fluorescence maps showing the elemental distribution of P (red), Al (green), and Si (blue) and corresponding P K-edge XANES spectra collected at SSRL beamline 14-3 for the Hagerstown soil.
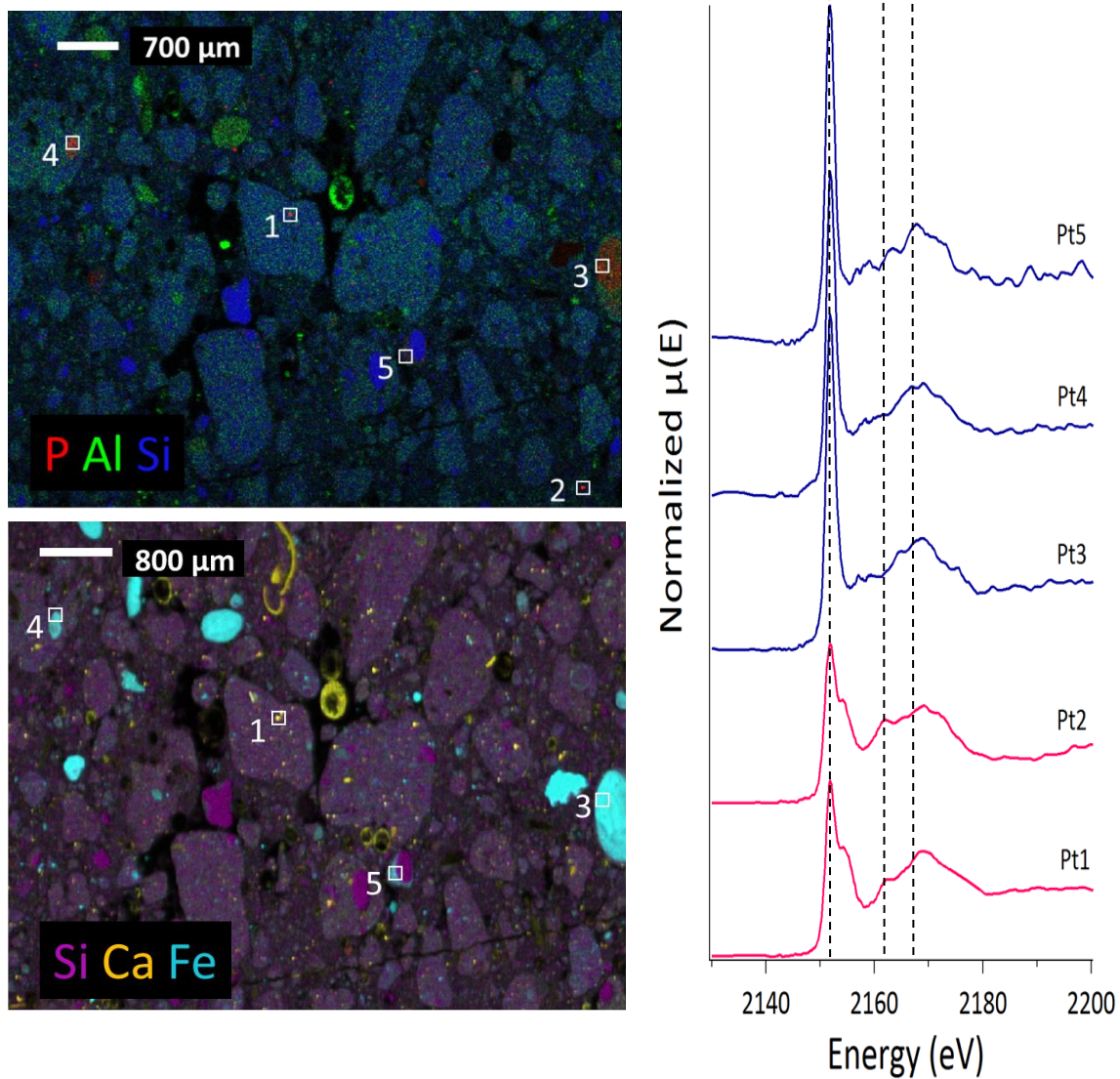
Figure 2.7. Tender-energy X-ray fluorescence maps showing the elemental distribution of P (red), Al (green), and Si (blue) and corresponding P K-edge XANES spectra collected at SSRL beamline 14-3 for the Berks soil.
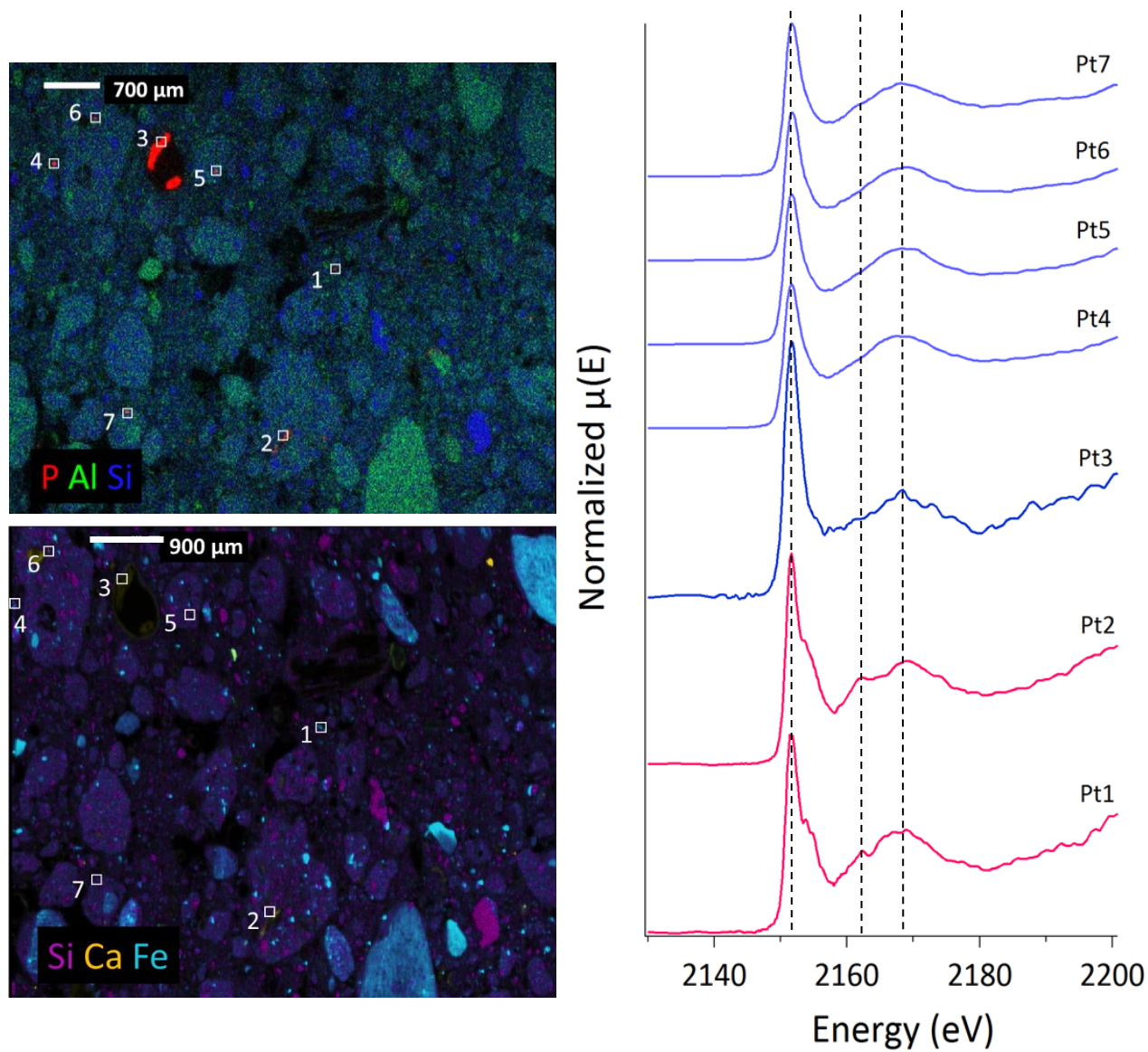
REFERENCES

Abdala, D.B., P.A. Northrup, F.C. Vicentin, and D.L. Sparks. 2015a. Residence time and pH effects on the bonding configuration of orthophosphate surface complexes at the goethite/water interface as examined by extended x-ray absorption fine structure (EXAFS) spectroscopy. J. Colloid. Interf. Sci. 442:15-21.

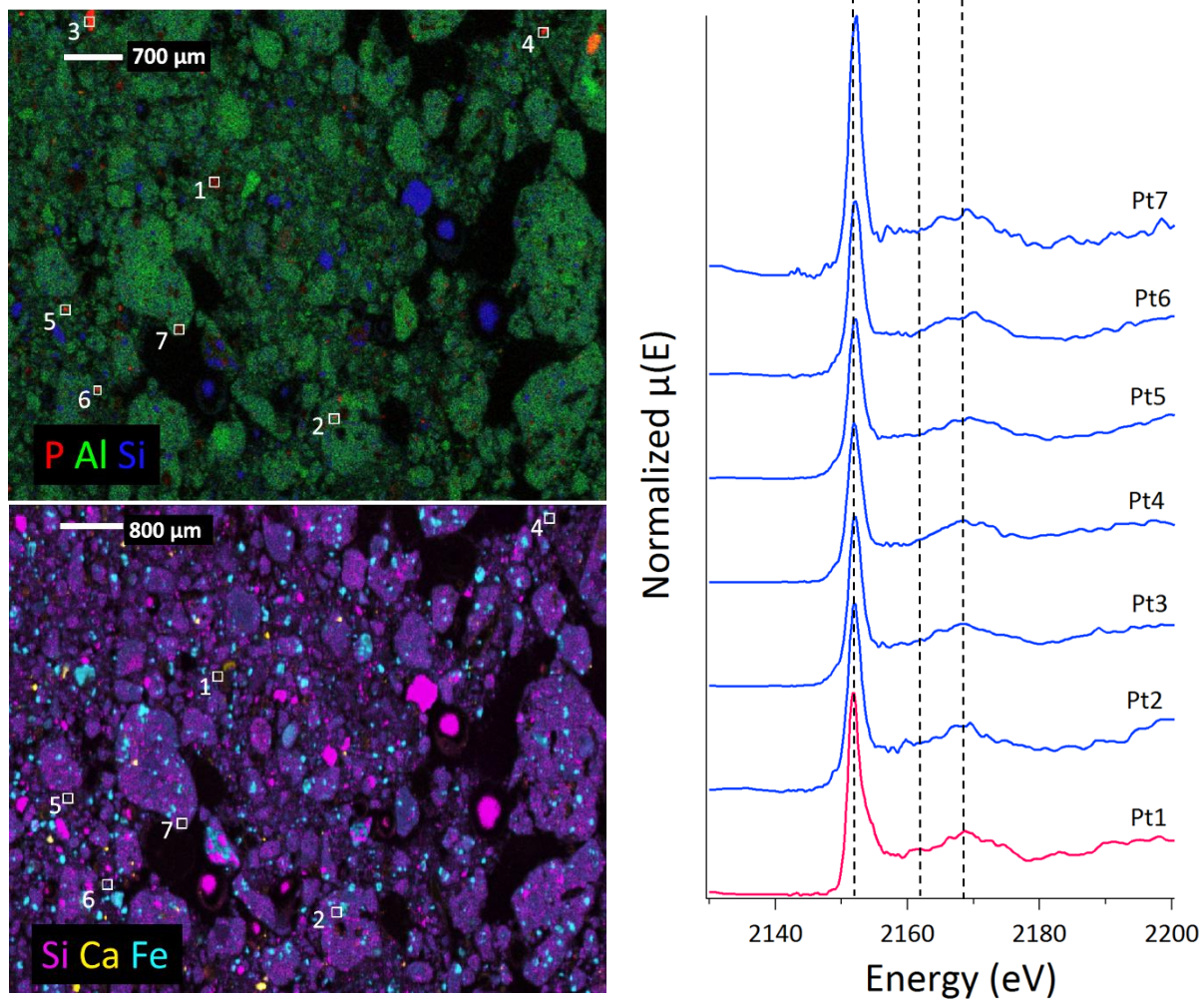Abdala, D.B., P.A. Northrup, Y. Arai, and D.L. Sparks. 2015b. Surface loading effects on orthophosphate surface complexation at the goethite/water interface as examined by extended x-ray absorption fine structure (EXAFS) spectroscopy. J. Colloid. Interf. Sci. 437:297-303.

Adeli, A., H. Tewolde, M.W. Shankle, T.R. Way, J.P. Brooks, and M.R. McLaughlin. 2013. Runoff quality from no-till cotton fertilized with broiler litter in subsurface bands. J. Environ. Qual. 42:284-291.

Arai, Y., and K.J. Livi. 2012. Underassessed phosphorus fixation mechanisms in soil sand fraction. Geoderma. 192:422-429.

Ajiboye, B., O.O. Akinremi, Y. Hu, and A. Jürgensen. 2008. XANES speciation of phosphorus in organically amended and fertilized Vertisol and Mollisol. Soil Sci. Soc. Am. J. 72:1256-1262.

Beauchemin, S., D. Hesterberg, J. Chou, M. Beauchemin, R.R. Simard, and D.E. Sayers. 2003. Speciation of phosphorous-enriched agricultural soils using X-ray absorption near-edge structure spectroscopy and chemical fractionation. J. Environ. Qual. 32:1809-1819.

Brandes, J.A., E. Ingall, and D. Paterson. 2007. Characterization of minerals and organic phosphorus species in marine sediments using soft X-ray fluorescence spectromicroscopy. Mar. Chem. 103:250-265.

Cade-Menun, B., and C.W. Liu. 2013. Solution phosphorus-31nuclear magnetic resonance spectroscopy of soils from 2005 to 2013: a review of sample preparation and experimental parameters. Soil Sci. Soc. Am. J. 78:19-37.

Del Nero, M., C. Galindo, R. Barillon, E. Halter, and B. Madé. 2010. Surface reactivity of α-Al$_2$O$_3$ and mechanisms of phosphate sorption: *In situ* ATR-FTIR spectroscopy and ζ potential studies. J. Colloid Interf. Sci. 342:437-444.

Environmental Protection Agency (EPA). 1995. EPA method 3050b: Acid digestion of sediments, sludges, and soils. In Test Methods for Evaluating Solid Waste, 3rd update. United States Environmental Protection Agency, Washington, D.C.

Frisia, S., A. Borsato, R.N. Drysdale, B. Paul, A., Grieg, and M. Cotte. 2012. A re-evaluation of the paleoclimatic significance of phosphorous variability in speothems revealed by high-resolution synchrotron micro XRF mapping. Clim. Past. 8:2039-2051.

Giguet-Covex, C., J. Poulenard, E. Chalmin, F. Arnaud, C. Rivard, J.-P. Jenny, and J.-M. Dorioz. 2013. XANES spectroscopy as a tool to trace phosphorus transformation during soil genesis and mountain ecosystem development from lake sediments. Geochim. Cosmochim. Ac. 118:129-147.

Hesterberg, D., W. Zhou, K.J. Hutchison, S. Beauchemin, and D.E. Sayers. 1999. XAFS study of adsorbed and mineral forms of phosphate.

Ingall, E.D., J.A. Brandes, J.M. Diaz, M.D. de Jonge, D. Paterson, I. McNulty, W.C. Elliot, and P. Northrup. 2011. Phosphorus K-edge XANES spectroscopy of mineral standards. J. Synchrotron Radiat. 18:189-197.

Jackson, M.L., C.L. Lim, and L.W. Zelzany. 1986. Oxides, hydorxides, and aluminosilicates. pg. 101-150. In A. Klute (ed.) Methods of Soil Analysis. Part 1. SSSA and ASA, Madison, WI.

Kar, G., D. Peak, J.J. Schoenau. 2012. Spatial distribution and chemical speciation of soil phosphorus in a band application. Soil Sci. Soc. Am. J. 76:2297-2306.

Khare, N., D. Hesterberg, S. Beauchemin, and S. Wang. 2004. XANES determination of adsorbed phosphate distribution between ferrihydrite and boehmite in mixtures. Soil Sci. Soc. Am.

Kizewski, F., Y. Liu, A. Morris, and D. Hesterberg. 2011. Spectroscopic approaches for phosphorus speciation in soils and other environmental systems. J. Environ. Qual. 40:751-766.

Kunze, G.W., and J.B. Dixon. 1986. Pretreatment for mineralogical analysis. pg. 91-100. In A. Klute (ed.) Methods of Soil Analysis. Part 1. SSSA and ASA, Madison, WI.

Lamba, J., P. Srivastava, T.R. Way, S. Sen, C.W. Wood, and K.H. Yoo. 2013. Nutrient loss in leachate and surface runoff from surface-broadcast and subsurface-banded broiler litter. J. Environ. Qual. 42:1547-1582.

Li, W., X. Feng, Y. Yan, D.L. Sparks, and B. Phillips. 2013. Solid-state NMR spectroscopic study of phosphate sorption mechanisms on aluminum (hydr)oxides. Environ. Sci. Technol. 47:8308-8315.

Lombi, E., K.G. Scheckel, R.D. Armstrong, S. Forrester, J.N. Cutler, and D. Paterson. 2006. Speciation and distribution of phosphorus in a fertilized soil: a synchrotron-based investigation. Soil Sci. Soc. Am. J. 70:2038-2048.

Luengo, C., M. Brigante, J. Antelo, and M. Avena. 2006. Kinetics of phosphate adsorption on goethite: comparing batch adsorption and ATR-IR measurements. J. Colloid Interf. Sci. 300:511-518.

Manceau, A., B. Lanson, M.L. Schlegel, J.C. Hargé, M. Musso, L. Eybert-Bérard, J. Hazeman, D. Chateigner, and G.M. Lamble. 2000. Quantitative Zn speciation in smelter-contaminated soils by EXAFS spectroscopy. Am. J. Sci. 300:289-343.

Northeast Coordinating Committee. 2011. Recommended soil testing procedures for the northeastern United States. Northeast Regional Bulletin 493. Agricultural Experiment Station, University of Delaware, Newark, DE.

Parfitt, R.L., R.J. Atkinson, and Roger C. Smart. 1975. The mechanism of phosphate fixation by iron oxides. Soil Sci. Soc. Am. J. 39:837-841.

Peak, D., J.T. Sims, and D.L. Sparks. 2002. Solid-state speciation of natural and alum-amended poultry litter using XANES spectroscopy. Environ. Sci. Technol. 36:4253-4261.

Piersynski, G.M., T.J. Logan, S.J. Traina, and J.M. Bigham. 1990. Phosphorus chemistry and mineralogy in excessively fertilized soils: Quantitative analysis of phosphorus-rich particles. Soil Sci. Soc. Am. J. 54:1576-1583.

Ravel, B., and M. Newville. 2005. Athena, Artemis, Hephaestus: Data analysis for x-ray absorption spectroscopy using IFEFFIT. J. Synchrotron Radiat. 12:537-541.

Rouff, A.K., S. Rabe, M. Nachtegaal, and F. Vogel. 2009. X-ray absorption fine-structure study of the effect of protonation and disorder and multiple scattering in phosphate solutions and solids. J. Phys. Chem. 113:6895-6903.

Sallade, Y.E., and J.T. Sims. 1997 Phosphorus transformations in the sediments of Delaware's agricultural drainageways: I. Phosphorus forms and sorption. J. Environ. Qual. 26:1571-1579.

Sato, S., D. Solomon, C. Hyland, Q.M. Ketterings, and J. Lehmann. 2005. Phosphorus speciation in manure and manure-amended soils using XANES spectroscopy. Environ. Sci. Technol. 39:7485-7491.

Schefe, C.R., P. Kappen, and P.J. Pigram. 2011. Carboxylic acids affect sorption and micro-scale distribution of phosphorus in an acidic soil. Soil Sci. Soc. Am. J. 75:35-44.

Sharpley, A.N., R.W. McDowell, and P.J.A. Kleinman. 2004. Amounts, forms, and solubility of phosphorus in soils receiving manure. Soil Sci. Soc. Am. J. 68:2048-2057.

Shober, A.L., D.L. Hesterberg, J.T. Sims, and S. Gardner. 2006. Characterization of phosphorus species in biosolids and manures using XANES spectroscopy. J. Environ. Qual. 35:1983-1993.

Shober, A.L., and J.T. Sims. 2007. Integrating phosphorus source and soil properties into risk assessments for phosphorus loss. Soil Sci. Soc. Am. J. 71:551-560.

Webb, S.M. 2005. SIXpack: A graphical user interface for XAS analysis using IFEFFIT. Physica Scripta. T115:1011-1014.

Whittig, L.D., and W.R. Allardice. 1986. X-ray diffraction techniques. pg. 331-375. In A. Klute (ed.) Methods of Soil Analysis. Part 1. SSSA and ASA, Madison, WI.

Chapter 3

PHOSPHORUS DESORPTION FROM HIGH P MID-ATLANTIC SOILS

3.1 Introduction

Phosphorus (P) sequestration and excess are concomitant problems in agricultural soils of the Mid-Atlantic region. When soil test P concentrations are below agronomic optimum, availability of P to crops is often limiting in the highly weathered, low pH soils of the Mid-Atlantic, due to strong retention of P by aluminum (Al) and iron (Fe) oxides. Conversely, excessive application of P fertilizer and manure has caused a build-up of P in soils to concentrations that exceed agronomic optimum; this excess P is susceptible to loss through runoff and leaching processes. Elevated levels of P in aquatic systems has led to eutrophication in major watersheds, including the Chesapeake Bay in the Mid-Atlantic region of the United States. Eutrophication can result in decreased levels of dissolved oxygen and excessive algae growth, threatening drinking, recreational, and industrial water supplies.

Regulations for P management in the Mid-Atlantic have become more stringent in recent years due to the contribution of agricultural soils to nutrient runoff into the Chesapeake Bay (Sharpley et al., 2013). Agriculture is currently the largest source of nonpoint pollution entering the Chesapeake Bay, accounting for an estimated 50% of P entering the watershed (Chesapeake Bay Foundation, 2012). The concentrated poultry industry in the Mid-Atlantic region has exacerbated excess P loading in soils. Fertilizer recommendations for poultry litter application were historically based on N content, leading to an over-application of P to soil.

57

While surface runoff has long been considered the primary pathway for P loss in agricultural systems, subsurface leaching can be a major contributor to P loss in sandy soils, soils with high OM, and soils with excessive P loading (Sims et al., 1998). Subsurface P losses to surface waters are often accelerated in artificial drainage systems (Sims et al., 1998). Low water tables and coarse-textured soils in the Mid-Atlantic increase the susceptibility to P loss through subsurface pathways.

Many states within the Chesapeake Bay watershed have made significant progress in reducing P loss from agriculture, but cannot completely eliminate P pollution entering the Bay. Identifying methods to reduce pollution from nonpoint agricultural sources will rely on increased understanding of P chemistry in soils. Sorption processes play key roles in regulating P transport of dissolved and particulate P in the environment. Soil properties such as pH, mineralogy, and organic matter content are major controllers of desorption and adsorption processes. The objective of this study is to examine agricultural soils from the Mid-Atlantic region with a variety of chemical and physical properties to assess the lability of P. Sequential fractionation and batch desorption studies were used to assess P retention soils with high total P concentrations.

3.2   Materials and Methods

3.2.1   Soil Characterization

Soils from three agricultural fields within the Mid-Atlantic region with high total P (>900 mg kg^{-1}) loadings were selected to evaluate soil P speciation. Soil chemical and physical properties are referenced in Table 3.1. Soils included a Mullica (coarse-loamy,

siliceous, semiactive, acid, mesic Typic Humaquepts)-Berryland (sandy, siliceous, mesic Typic Alaquods) sandy loam complex, a Davidson (fine, kaolinitic, thermic Rhodic Kandiudults) silty clay, and a Hagerstown (fine, mixed, semiactive, mesic Typic Hapludalfs) silty clay loam. Samples were collected from the top 5 cm of soil. A more detailed description of Davidson, Hagerstown, and Berks soil samples can be found in Shober and Sims (2006). The Mullica-Berryland soil is currently managed under grain production and historically received high applications of broiler litter.

Prior to analysis, soil samples were air-dried, ground, and sieved to <2 mm particle size. Characterization of pH, organic matter content, particle-size, Mehlich3-extractable element content, and total digests for P, Al, and Fe was performed according to standard methods at the University of Delaware Soil Testing Laboratory (Sims and Wolf, 2011). An ammonium-oxalate extraction was completed according to procedures in Jackson et al. (1986) to estimate amorphous Al- and Fe- oxide content. Following Mehlich3-extractions, total digests, and ammonium-oxalate extractions, inductively coupled plasma-atomic emission spectroscopy was used to measure elemental concentrations.

3.2.2   Sequential Extractions

Sequential extractions were used to estimate the amount of P in various inorganic fractions. It should be noted that P in extracts is operationally-defined, and sequential extractions do not provide direct evidence of P speciation. For an estimate of loosely-bound, Al-bound, Fe-bound, reductant-soluble P, and Ca-bound P, a sequential extraction procedure based on Chang and Jackson (1957) was followed according to methods outlined in Zhang and Kovar (2000). This method for sequential fractionation

was chosen to compare to results for μ-XANES analysis, which is primarily used to identify inorganic P species. The first step of the sequential fractionation procedure used an ammonium chloride (NH_4Cl) extract to remove loosely-sorbed P. This was followed by ammonium fluoride (NH_4F) to remove extractable Al-bound P, sodium hydroxide (NaOH) extraction to remove Fe-bound P, sodium citrate-sodium dithionite-sodium bicarbonate (DCB) extraction to remove reductant-soluble P, and sulfuric acid (H_2SO_4) to dissolve Ca phosphate minerals. Supernatant was collected following each extraction, and the ammonium molybdate method (Murphy and Riley, 1962) followed by analysis with UV-VIS spectroscopy or ICP-OES was used to colorimetrically assess P concentration in extracts.

3.2.3 Phosphorus Desorption

Batch desorption studies were used to assess P retention in soils and followed methods outlined in Sparks et al. (1996). Electrolyte solutions of 10 mM KCl, 0.1 mM Na_3AsO_4, 1 mM Na_3AsO_4, and 0.1 M HNO_3 were used to desorb phosphate. The 10 mM KCl solution was used to represent background soil electrolyte, arsenate was chosen as a replacement anion due to its chemical similarity to phosphate, and HNO_3 was used to represent acidic weathering environments in soil (e.g., acid rain). Four grams of soil were weighed into 250-mL Nalgene® bottles, and 200 mL of electrolyte solution was added. Batch reactors were shaken at 120 rpm over a 3-d period, and 5-mL samples were withdrawn at time intervals of 1, 2, 3, 6, 12, 24, 48, and 72 h. Samples were filtered with Millipore® syringe-filters to 0.22 μm and measured with ICP-MS for total As concentration. Original soil pH was maintained during desorption reactions for KCl and Na_3AsO_4 solutions by adjusting with 0.1 M HCl or 0.1 M NaOH after each sample was

taken. A pH of 4 was maintained for desorption experiments with HNO_3. Batch reactions were performed in duplicate for each sample and each electrolyte solution.

3.3   Results and Discussion

3.3.1   Sequential Extractions

In the Mullica-Berryland soil, 31 mg P kg^{-1} soil was NH_4Cl-extractable, which represents loosely-sorbed soil P (Fig 3.1). A large fraction of Al-associated P is predicted based on the high NH_4F-extractable content of over 900 mg P kg^{-1} soil. This is in agreement with Abdala et al. (2015), who found that up to 44% of total P was present in the Al-bound P fraction. Minor concentrations of NaOH-extractable (53.7 mg kg^{-1}) and DCB-extractable P (22 mg kg^{-1}) were observed in the Mullica-Berryland soil. Results from μ-XANES analysis in chapter two indicate that Ca phosphate minerals, Al-oxide sorbed P, and Fe-oxide sorbed phosphate species are present in the Mullica-Berryland soil. Calcium phosphate minerals were the most frequently detected P species with μ-XANES, but only 43 mg P kg^{-1} was extracted in the H_2SO_4 step of sequential fractionation, the extraction which represents Ca-associated P. Al-sorbed species may have been more difficult to detect with μ-XANES because they are distributed more diffusely throughout the soil. The Mullica-Berryland soil is 78% sand, and much of the sorbed P is probably present in metal-oxide coatings on sand particles. Approximately 14% of P was unaccounted for with sequential extractions and may represent P fractions that are more resistant to degradation.

Loosely-sorbed P was below detection for the Davidson soil, and 65 mg kg^{-1} was considered Al-associated. Iron-bound phosphate appears to be the dominant P form in

the Davidson soil, with 359 mg kg^{-1} present in the NaOH extractant and 85.5 mg kg^{-1} present in the DCB extractant. This is in agreement with results in chapter 2, in which 5 out of 7 hotspots analyzed were in Fe-oxide sorbed forms and one hotspot was in Ca phosphate form. Concentration of P followed the order NaOH>H_2SO_4>DCB>NH_4F>NH_4Cl. Approximately half of the P in the Davidson soil was not accounted for in sequential extractions, indicating that P is extremely recalcitrant in the Davidson soil.

For the Hagerstown soil, P was also contained primarily in the Fe-associated fractions. Less than 0.1% of P was extracted with NH_4Cl, and concentration of P in extracts followed the order NaOH>NH_4F>DCB>H_2SO_4>NH_4Cl. Micro-XANES spectra collected for the Hagerstown soil in chapter 2 revealed the presence of Ca phosphate and oxidized Fe phosphate minerals, which would be represented in the H_2SO_4-extractable P pools and DCB-extractable, respectively.

Sequential extractions were used to give an approximation of inorganic P speciation in soil and do not reflect the precise speciation of soil P. Concentration of P in the NaOH extract, which represents Fe association, was highest for both the Davidson and Hagerstown. Sequential extractions indicate that P is primarily associated with Fe or Al in each of the three soils examined in this study. The Mullica-Berryland soil, which is the coarsest textured-soil with low amorphous Fe and Al oxide content, contained the greatest fraction of loosely-sorbed P and Mehlich3-extractable P. Concentration of P in various sequential extracts is not representative of major species identified with μ-XANES. Results are partially explained by the easier detection of P with μ-XANES in discrete, P-rich particles.

3.3.2 Phosphorus Desorption

For each soil type, P desorption was characterized by an initial rapid desorption over the first 12 h, followed by a slower desorption reaction from 12 to 72 h (Fig 3.2 and Fig 3.3). It is not uncommon to observe a biphasic desorption of phosphate from soil minerals (Arai and Sparks, 2007). Kuo and Lotse (1973) observed that the majority of phosphate was desorbed from metal oxide surfaces after a 24-h extraction in various electrolyte solutions. For desorption reactions at the original soil pH (i.e., KCl and Na_3AsO_4 solutions), the percentage of P desorbed increased with increasing concentrations of arsenate in solution.

For the Mullica-Berryland soil, approximately 10% (120 mg kg^{-1}) of P was desorbed with 10 mM KCl and up to 14% (180 mg kg^{-1}) was desorbed with 1 mM Na_3AsO_4 solution (Fig 3.2). Total P desorption after 72 h in background electrolyte solution of 10 mM KCl is high enough to be considered excessive in Delaware soils according to Mehlich3 extractions, which is a stronger extractant of P (Sims et al., 2002). The amount of P desorbed with 1 mM Na_3AsO_4 and 0.1 M HNO_3 was roughly equal. It is surprising that only 14% of P was desorbed in pH 4 HNO_3 since Mehlich3-extractable P makes up almost half of total P (Table 3.1). The Mullica-Berryland soil had the lowest amount of ammonium-oxalate extractable Fe and Al and highest soil P content of the evaluated soils. Direct spectroscopic evidence demonstrates that P is more susceptible to desorption at high soil solution P concentrations (Abdala et al., 2015b).

For the Davidson soil, less than 1 mg kg^{-1} of P was desorbed with 10 mM KCl and only 6 mg kg^{-1} is desorbed in 0.1 mM arsenate solution. Results for low desorption in KCl are in agreement with sequential extraction data, which indicated that no P was loosely-sorbed. Eight times as much P (50 mg kg^{-1}) was desorbed with 1 mM arsenate compared

to 0.1 mM arsenate, but only accounts for approximately four percent of total P. In pH 4 HNO_3 solution, 2.5 mg kg^{-1} was released. The low percentage of P desorbed for the Davidson soil, even in solutions with high arsenate concentration, may be explained by the large Fe- and Al-oxide content of this soil. This soil has an 11.2% Fe content and a 2.6% Al content and contains 1390 and 1284 mg kg^{-1} ammonium-oxalate extractable concentrations of Fe and Al, respectively. It also has the largest percentage of clay (>50%), and the high surface area of this soil contributes additional sorption sites for P. Speciation analysis with μ-XANES paired with sequential extraction analysis revealed that the majority of P in the Davidson soil is associated with Fe-oxides. Desorption with higher concentrations of arsenate may reveal that a larger percentage of P is retained through inner-sphere complexation. It is predicted that P Fe- and Al-minerals or surface precipitates also contribute to P speciation based of the low availability of P in these soils.

For the Hagerstown soil, less than 1% (8 mg kg^{-1}) of total P was desorbed in KCl and approximately 4% (43 mg kg^{-1}) was desorbed in 1 mM arsenate solution. Less P (32 mg kg^{-1}) was desorbed in HNO_3 solution than was desorbed with 1 mM arsenate. Speciation analysis with μ-XANES revealed that apatite and strengite dominate P speciation in the Hagerstown soil. Although apatite and strengite are soluble at pH 4, dissolution in 0.1 M HNO_3 may not have occurred for the sampling times used in this study (<72 h). This soil also had a high concentration of amorphous Fe and Al oxides based on ammonium-oxalate extractions (1450 and 1150 mg kg^{-1}, respectively).

The high recalcitrance of P in Davidson and Hagerstown soil can be partially explained by the high amorphous Fe- and Al-oxide content in these soils. Low percentages of total P desorption have been observed in previous studies investigating Fe- and Al- oxides. At pH values below 6.5, most Fe- and Al-oxides are positively charged

and have greater sorption capacity for phosphate. For example, total P desorption was lower for ferrihydrite at pH 4 than pH 7, even though P loading was higher for ferrihydrite at pH 4 in experiments performed by Arai et al. (2007). Beauchemin et al. (1999) observed more rapid desorption of P for soils with low ammonium-oxalate extractable Al content. Abdala et al. (2015a) report that 1.7 to 2.4% of ammonium-oxalate extractable P was desorbed after a 1-h stirred-flow desorption experiment in 1 M NH_4Cl in manure-amended acidic soils.

The residence time of P in these soils is likely an additional contributor to P retention. Over time, diffusion processes, surface precipitation, and formation of higher-energy surface complexes can limit potential P desorption from soil. Arai and Sparks (2007) observed a decrease from 4.8 to 0.9% total P desorbed when aging of ferrihydrite-adsorbed phosphate was increased from 2 days to 10 months in stirred-flow experiments with 0.1 M NaCl at pH 4; for the same experiment at pH 7, P desorption was reduced from 10.1 to 3.8% for aging times of 2 days and 19 months, respectively.

3.4   Conclusions

Sequential extractions indicate that P is largely associated with Al- and Fe-oxides in soil. Results from sequential extracts is not representative of major species identified with μ-XANES and support conclusions in chapter 2 that P species are more easily-identified with μ-XANES in discrete, P-rich particles. Phosphate desorption increased with increasing concentration of competing ions in solution for all soils. Soils with the highest amorphous Al- and Fe-oxide content corresponded to soils with the lowest concentration of P desorption and the greatest effect of competing anions in solution.

Table 3.1. Characterization analysis of Mullica-Berryland, Davidson, Hagerstown, and Berks soils.

Soil Series	pH	Sand	Silt	Clay	OM[1]	Total Fe	Total Al	Al_{ox}[2]	Fe_{ox}[3]	M3-P[4]	Total P
		————%————				———— g kg^{-1}————		————— mg kg^{-1}—————			
Mullica-Berryland	4.2	78.4	8.2	13.4	38	1.6	6.3	549	507	668.3	1256
Davidson	6.4	2.3	50.4	47.3	31	112.2	60.9	1284	1390	27.4	1216
Hagerstown	5.6	1.5	62.9	35.6	36	25.9	20.5	1146	1453	111.9	986

[1] Organic matter content

[2] Ammonium-oxalate extractable Al

[3] Ammonium-oxalate extractable Fe

[4] Mehlich3-extractable P

Figure 3.1. Sequential Extraction results for Mullica-Berryland, Davidson, and
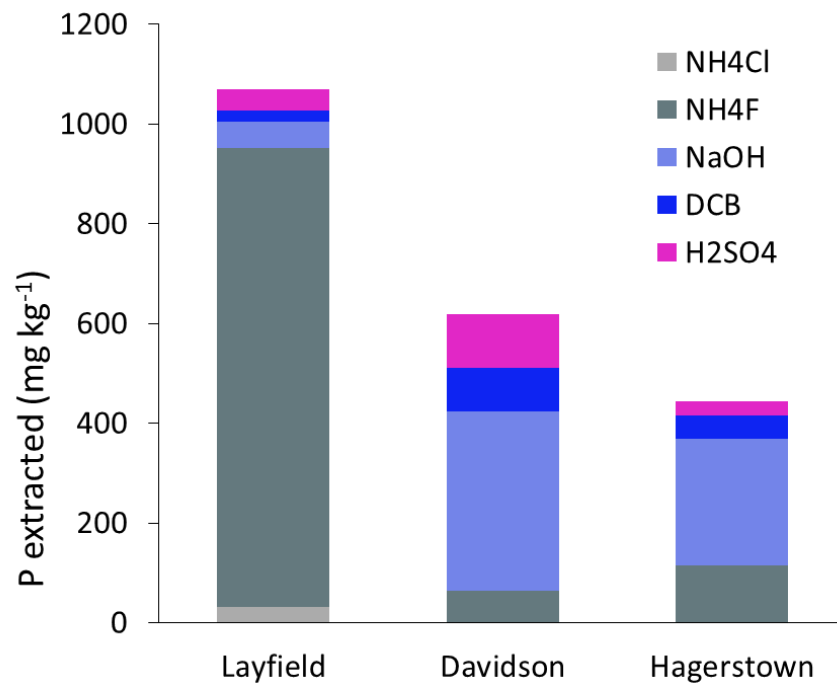
Hagerstown.

Figure 3.2 Fraction of total phosphate and concentration of phosphate released over a

3-d desorption experiment in 10 mM KCl, 0.1 mM Na_3AO_4, and 1 mM Na_3AO_4 for

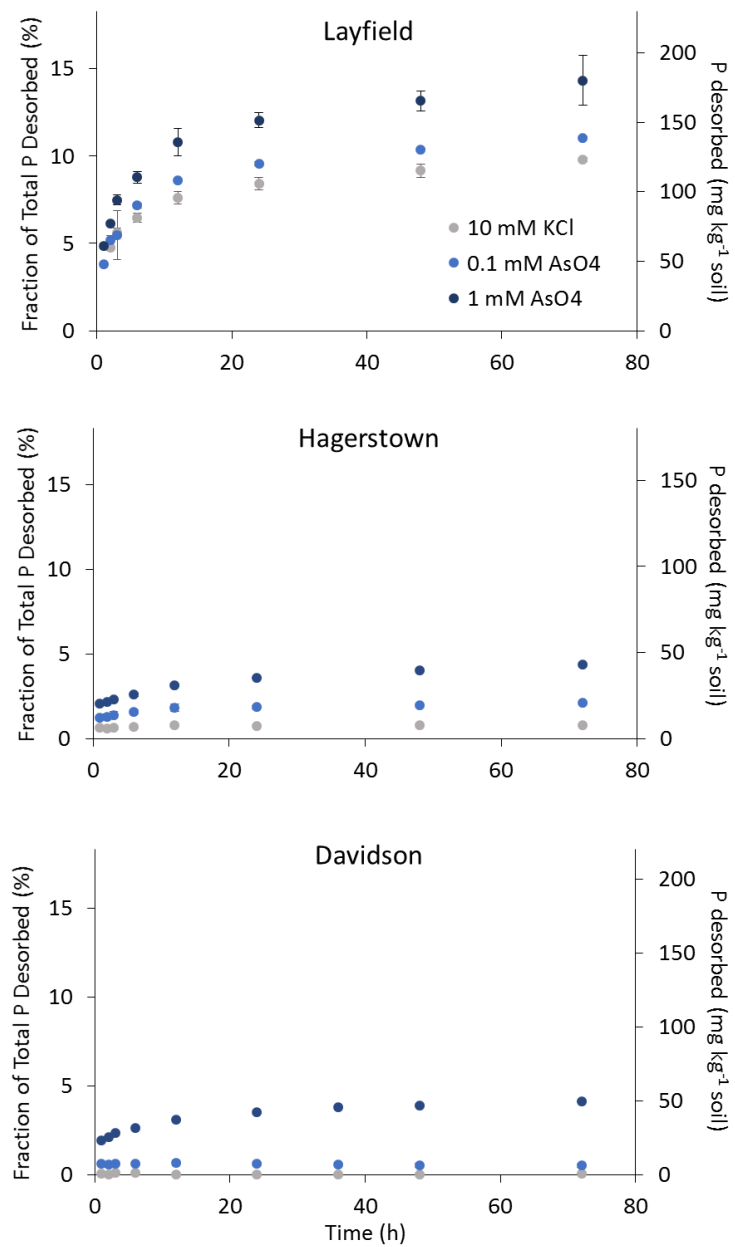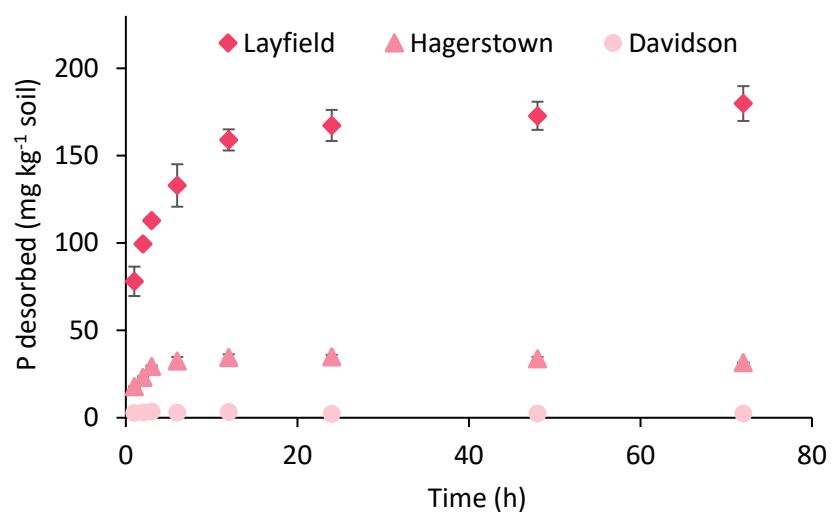Mullica-Berryland, Hagerstown, and Davidson soils.

Figure 3.3 Phosphate release over a 3-d desorption experiment in 0.1 M HNO_3 at pH 4

for Mullica-Berryland, Hagerstown, and Davidson soils.

REFERENCES

Abdala, D.B., P.A. Northrup, Y. Arai, and D.L. Sparks. 2015a. Surface loading effects on orthophosphate surface complexation at the goethite/water interface as examined by extended x-ray absorption fine structure (EXAFS) spectroscopy. J. Colloid. Interf. Sci. 437:297-303.

Abdala, D.B., I. Ribeiro de Silva, L. Vergütz, and D.L. Sparks. 2015b. Long-term manure application effects on phosphorous speciation, kinetics, and distribution in highly weathered agricultural soils. Chemosphere. 119:504-514.

Arai, Y., and D.L. Sparks. 2007. Phosphate reaction dynamics in soils and soil components: a multiscale approach. Adv Agron. 94:135-179.

Beauchemin, S., R.R. Simard, and D. Cluis. 1996. Phosphorus sorption-desorption kinetics of soil under contrasting land uses. J. Environ. Qual. 25:1317-1325.

Chang, S.C., and M. L. Jackson. 1957. Fractionation of soil phosphorus. Soil Sci. 84:133-144.

Chesapeake Bay Foundation. 2012. The economic argument for cleaning up the Chesapeake Bay and its rivers. Chesapeake Bay Foundation, Annapolis, MD. Jackson, M.L., C.L. Lim, and L.W. Zelzany. 1986. Oxides, hydorxides, and aluminosilicates. pg. 101-150. In A. Klute (ed.) Methods of Soil Analysis. Part 1. SSSA and ASA, Madison, WI.

Kuo, S., and E.G. Lotse. 1973. Kinetics of phosphate adsorption and desorption by hematite and gibbsite. Soil Sci. 116:400-406.

McGechan, M.B., and D.R. Lewis. 2002. Sorption of phosphorus by soil, part 1: principles, equations and models. Biosyst. Eng. 82:1-24.

Murphy, J. and J.P. Riley. 1962. A modified single solution method for the determination of phosphate in natural waters. Analytica Chemica Acta. 27:31-36.

Ryden, J.C., and J.K. Syers. 1977. Desorption and isotopic exchange relationships of phosphate sorbed by soils and hydrous ferric oxide gel. J. Soil Sci. 28:596-609.

Shang, C., J.W.B. Stewart, and P.M. Huang. 1992. pH effect on kinetics of adsorption of organic and inorganic phosphates by short-range ordered aluminum and iron precipitates. Geoderma. 53:1-14.

Sharpley, A., H.P. Jarvie, A. Buda, L. May, B. Spears, and P. Kleinman. 2013. Phosphorus legacy: Overcoming the effects of past management practices to mitigate future water quality impairment. J. Environ. Qual.

Shober, A.L., and J.T. Sims. 2007. Integrating phosphorus source and soil properties into risk assessments for phosphorus loss. Soil Sci. Soc. Am. J. 71:551-560.

Sims, J.T., R.R. Simard, and B.C. Joern. 1998. Phosphorous loss in agricultural drainage: Historical perspective and current research. J. Environ. Qual. 27:277-293.

Sims, J.T. and A. Wolf. 2011. Recommended soil testing procedures for the northeastern United States. Northeast Regional Bulletin 493. Agricultural Experiment Station, University of Delaware, Newark, DE.

Sims, J.T, R.O. Maguire, A.B. Leytem, K.L. Gartley, and M.C. Pautler. 2002 Evaluation of Mehlich 3 as an agri-environmental soil phosphorus test for the Mid-Atlantic United States of America. Soil Sci. Soc. Am. J. 66:2016-2032.

Sparks, D.L., S.E. Fendorf, C.V. Toner, and T.H. Carski. 1996. Kinetic methods and measurements. In: D.L. Sparks (ed.) Methods of Soil Analysis: Part 3. SSSA and ASA, Madison, WI.

Zhang, H., and J.L. Kovar. 2000. Phosphorus Fractionation. pg. 50-59. In G.M. Pierzynski (ed.) Methods of phosphorus analysis for soils, sediments, residuals, and waters. North Carolina State University, Raleigh, NC.

Chapter 4

ARSENIC REACTIVITY AND BIOAVAILABILITY IN FORMER ORCHARD SOILS

4.1   Introduction

Lead arsenate was a commonly used pesticide in fruit tree orchards from the 1890s to 1940s (Udovic and McBride, 2012). Arsenic (As) is a known toxin and carcinogen, and soil As concentrations exceeding 100 mg kg^{-1} have been observed in former peach and apple orchards in the Pacific Northwest, New York State, and Pennsylvania (Davenport and Peryea, 1991; Jones and Hatch, 1937; Merwin et al., 1994). Delaware was among the leading producers of peaches in the late 1800s, and over 4.5 million peach trees were in production in 1890 according to the U.S. agricultural census (Hedrick et al., 1917). Frequent lead arsenate applications at high concentrations during this time likely led to accumulation of As in orchard soils. Due to a disease called "peach yellows," the peach industry drastically declined in the early 1900s, and the number of peach trees in the state decreased to 1.2 million by 1910. Many previous orchards have since been converted to cropland but are now being sold for residential and public use, posing a lingering threat of As-related illnesses to the public; therefore, a comprehensive study of the concentrations and toxicity of As in former Delaware orchard soils is necessary to evaluate the associated risks to human and environmental health in the state of Delaware.

Regulatory limits for soil As have been established by federal and state agencies to protect human health. The Delaware Department of Natural Resources and Environmental Control (DNREC) has established a cleanup standard for soil As concentration of 11 mg kg^{-1} in residential areas (DNREC, 2007). The Delaware cleanup

72

standard is higher than the EPA soil As screening level of 0.4 mg kg^{-1} since 11 mg kg^{-1} is the estimated background As concentration for Delaware soils. This concentration is also above the estimated median of 7.2 mg kg^{-1} for soils in the United States (Shacklette and Boerngen, 1984). Exposure estimates for soil contamination are based on total soil As, which assume that 100 percent of As is soluble and toxic. However, this assumption can overestimate risk for As contamination. The toxicity and bioavailability of soil As is dependent upon a number of factors, including As speciation (form) and soil properties. For example, the reduced form [As(III)] is more mobile and toxic than the oxidized form [As(V)] in soil (Cui and Weng, 2013). In addition, it is well-established that As forms inner-sphere complexes to metal oxide surfaces resulting in strong retention by Fe- and Al- oxides in soils (Fendorf et al., 1997; Yang et al., 2002; Beak et al., 2006). Factors such as pH, redox conditions, soil texture, organic matter (OM) content, and competitive ions also play key roles in As sequestration (Merry et al., 1983; Dixit and Hering, 2003; Bradham et al., 2011). Studies by the EPA have demonstrated that approximately 11 to 53 percent of total soil As is bioavailable to humans based on in vivo bioavailability studies in mice (Bradham et al., 2011).

The current study assesses speciation, transport, and bioavailability of soil As to predict its potential toxicity in Delaware soils. Soils from three former orchard sites in Delaware with elevated (>11 mg kg^{-1}) soil As concentrations were evaluated. Desorption studies were used to measure mobility of As in the environment under varying environmental conditions. Bioaccessibility studies were used to determine the portion of total soil As that is potentially toxic to humans after ingestion. Micro-scale X-ray fluorescence (XRF) and X-ray absorption near-edge spectroscopy (XANES) were used to determine the oxidation state and distribution of As within the soil. Soil characterization of metal(loid), Fe- and Al-oxide, and organic matter (OM) contents accompanied XANES

studies to assess soil As speciation. Numerous studies have been conducted to evaluate As transport and retention in former orchard soils (Jones and Hatch, 1937; Merry et al., 1983; Merwin et al., 1994; Peryea, 1991; Peryea and Creger, 1994), but to our knowledge, this is the first study to use synchrotron-based speciation techniques to assess As speciation. Data collected for As speciation, mobility, and bioavailability are presented to DNREC to guide safe and cost-effective strategies for remediation of As contaminated soils in Delaware.

4.2   Materials and Methods

4.2.1   Soil Sample Collection

Three historic orchard sites located in Newark, Camden, and Lewes, Delaware were selected for this study. The presence of a former orchard was confirmed via on aerial images collected from the Delaware Environmental Monitoring and Analysis Center (DEMAC, 2015) for Lewes, (Fig. 3.1), Newark (Fig. 3.2), and Camden (Fig. 3.3) locations. Soils at the Lewes site are primarily classified as Downer sandy loam, with smaller series components of Evesboro loamy sand and Greenwich loam. Soils at the Newark location are classified as Elsinboro silt loam, and soils at the Camden location are classified as Sassafrass sandy loam according to Web Soil Survey (2016). The Lewes and Newark sites were managed as cropland at the time of sampling, and the site at Camden was managed in ornamental turf. Approximately 20 soil cores per hectare were collected from 0 to 20 and 20 to 40 cm depths at each location and were combined to form composite samples. Three of these composite samples were collected for each location and depth as replicates. Two uncontaminated sites (Felton and Lincoln) with similar soil properties to the orchard sites were sampled as a control.

4.2.2   Soil Characterization

Prior to analysis, soils were air-dried, ground, and sieved (<2 mm). Organic matter (OM) content, pH, metal(loid) concentrations, cation exchange capacity (CEC), and Mehlich3-extracable nutrient concentrations were measured according to standard procedures at the University of Delaware Soil Testing Laboratory (Sims and Wolf, 2011). An ammonium oxalate-extraction was used to estimate amorphous Al and Fe oxide content according to procedures in Jackson et al. (1986). Microwave acid digestion per EPA method 3051b was used for total metal analyses of As, Pb, Fe, and Al (EPA, 1995). Following digestion, inductively coupled plasma atomic emission spectroscopy was used to measure total concentrations for Pb, Fe, and Al. Inductively coupled plasma mass spectrometry (ICP-MS) was used to measure total As concentration since this instrument has lower detection limits needed for As analysis of the soil extracts. Each analyses was completed for each composite sample for each location.

4.2.3   Arsenic Desorption

Desorption studies were used to comparatively assess the ability of soil to retain As. Stir-flow desorption kinetics studies followed methods outlined in Lafferty et al. (2010). One gram of soil sample was placed in a 20-mL stirred-flow reactor, and influent solutions of pH-adjusted 10 mM KCl, 0.1 mM KH_2PO_4, or 1 mM KH_2PO_4 were pumped at a flow rate of 1 mL per minute through the reactor with a peristaltic pump. The 10 mM KCl background electrolyte was used to represent a typical electrolyte concentration in soils, and the 0.1 mM KH_2PO_4 and 1 mM KH_2PO_4 were used to examine the effect of an environmentally-relevant competing ion for arsenate. The pH for influent solution was adjusted to reflect the soil pH and varied based on sampling location. Phosphate was chosen as a replacement anion due to its chemical similarity to As and environmental

relevance, since phosphorus (P) fertilizers were likely applied at sampling sites that were under crop production (i.e., Lewes and Newark sites). Effluent was collected in 5-mL increments in a fraction collector over a 24-h period. Samples were filtered to 22 μm and analyzed using ICP-MS to determine total As desorption over time.

4.2.4   Arsenic Bioavailability

To evaluate the bioavailability of soil As, an *in vitro* physiologically-based extraction test followed methods of Diamond et al. (2016) to simulate digestion in a human gastrointestinal tract. Soils were sieved to < 250 μm for this extraction to represent soil particles, which represents the size fraction most likely to be ingested by humans, particularly children. In this procedure, 100 mL of 0.4 M glycine solution at pH 1.5 was added to 1 g of soil (< 250 μm) and shaken for 1 h in a 37°C water bath. Following digestion, extracts were analyzed with ICP-MS to determine total As. Extracted As concentration was divided by total As to determine the percent *bioaccessible* As. Bioaccessible As from *in vitro* extraction studies is related by Equation 1 to relative bioavailable As determined from *in vivo* studies in mice by the US EPA (Diamond et al., 2016).

$$\% \ Relative \ Bioavailable \ Arsenic = \% \ Bioaccessible \ As \times 0.79 + 3\%$$
(Equation 1)

In vitro extractions are not likely to have an effect on As oxidation state. Beak et al. (2006) found that As was strongly sorbed to ferrihydrite, a common, highly reactive Fe oxide present in soils, via inner-sphere complexation both before and after an in vitro extraction test. They also did not observe any reduction of As(V) to As (III) during extraction.

4.2.5   Arsenic Speciation

Arsenic speciation with μ-XRF and μ XANES analyses was measured at the Stanford Synchrotron Radiation Lightsouce (SSRL) on beamline 2-3 operated at 3 GeV. Soil samples used for speciation analysis were loaded into EPO-TEK® epoxy resin, thin-sectioned to 30 μm at Spectrum Petrographics, and mounted to a high-purity quartz slide. The highest concentration samples (Lewes and Newark soils at 0-20 and 20-40 cm depths) were chosen for speciation analysis. X-ray fluorescence maps were collected at 12,000 eV to assess spatial distribution of As and Fe in soils. The X-ray beam was focused with Kirkpatrick-Baez mirrors to approximately 5-μm diameter step-size, and 20-ms dwell time per pixel was used. Arsenic hotspots were identified from μ-XRF maps for μ-XANES analysis at the As K-edge. Spectra were collected from 11.6-12.3 keV, with a 0.4 eV step size from the 11.85-11.90 keV. XANES spectra were successfully collected for five As hotspots in the Lewes soil at the 0-20 cm depth, six As hotspots in the Lewes soil at the 20-40 cm depth, five As hotspots for the Newark soil at the 0-20 cm, and three As hotspots for the Newark soil at the 20-40 cm depth. Two to three XANES spectra per As hotspot were collected and averaged to increase spectral quality. Replicate spectra for each hotspot were examined for shifts in edge location to ensure that no photoxidation of As(III) to As(V) resulted from incident X-rays.

Sam's MicroAnalysis Toolkit (Webb, 2005) was used to process μ-XRF maps and create As and Fe distribution images. Raw XANES spectra were averaged in Sixpack software (Webb, 2005). Pre- and post-edge background corrections and spectral alignment were completed in Athena (Ravel and Newville, 2005). The first peak of the second derivative was chosen as E0. Spectra collected from SSRL were compared to reference standards with a known composition to examine the oxidation state of As.

Standards of scorodite [As(V)], schneiderhonite [As(III)], and realgar (AsS) were collected at the Advanced Photon Source at beamline 13-ID.

4.3   Results and Discussion

4.3.1   Soil Characterization

Soil properties and Mehlich-3 extractable elements are presented in Table 4.1 and 4.2, respectively. Soil pH ranged from 5.6 to 6.2 and organic matter content ranged from 7.0 to 22.7 g kg^{-1} soil. Soils higher in OM had corresponding higher CEC values. All soils contain appreciable concentrations of ammonium-oxalate extractable Al and Fe, indicating a high amorphous Al- and Fe- oxide content. Ammonium-oxalate extractable Fe and Al was highest for soils at the Newark location.

Soil As and Pb concentrations in former orchard soils ranged from approximately 11.8 to 59.0 mg kg^{-1} soil and 25.9 to 116.5 mg kg^{-1} soil, respectively (Table 4.3). The three former orchard soils had As concentrations exceeding the DNREC cleanup level of 11 mg kg^{-1}. Soil As at the control locations at Felton and Lincoln were below 6 mg kg^{-1}. Soil Pb was well below the established EPA cleanup levels of 400 mg kg^{-1} in all former orchard and control sites; therefore, soil Pb was not considered a health risk at these locations.

The As:Pb ratio ranged from 0.35 to 0.51 in former orchard soils. In the Lewes and Newark soils, which are currently managed as cropland, As:Pb ratio was comparable to the ratio for lead arsenate of 0.36 (Table 4.3). Arsenic concentration and As:Pb ratios increase from the 0-20 to the 20-40 cm depth. The As:Pb ratio for the Camden soil decreases with depth. The downward leaching of As in the Lewes and Newark soil profiles may be attributed to competition with phosphate from P fertilizer application.

The Newark soil at 0-20 and 20-40 cm depths is considered optimum in Mehlich-3 extractable P, and additional P fertilizer would not be recommended according to Delaware soil testing standards (Sims et al., 2002). The Lewes soil is considered optimum in extractable P at the 0-20 cm depth and below optimum at the 20-40 cm depth according to Delaware soil testing standards. We suggest that some arsenate is exchanged with phosphate in the top soil depth and leached deeper into the soil profile, where arsenate is re-adsorbed. Several studies have observed leaching of soil As further into the soil profile in former orchard soils. Peryea and Creger (1994) observed increasing As:Pb ratio with increasing depth in a survey of 6 soils from Washington state former and current orchards. These soils were coarse-textured with low OM, similar to the Lewes and Camden soils in this study. Peryea and Creger (1994) attribute leaching of As to deeper soil layers to high sand content, low organic matter, and heavy irrigation at the former orchard sites. Similarly, Merry et al. (1983) report leaching of As into deeper soil layers in sandy oxides, with the greatest accumulation observed in the 23 to 28 cm depth; they did not observe movement of Pb into deeper soil layers even in sandy soils.

4.3.2   Arsenic Desorption

Results for stirred-flow desorption are presented in Fig 4.4. Desorption occurs rapidly during the first 60 min and levels off throughout the 24-h reaction for each soil. Approximately 7.1, 0.2, and 12.5% of total As is desorbed with 10 mM KCl after a 24-h reaction for the Lewes, Newark, and Camden soils, respectively. The percent of total As desorbed increases with increasing phosphate concentration in electrolyte solution. In 0.1 mM and 1 mM KH_2PO_4 solutions, approximately 18 and 53%, respectively, of total As was desorbed for the Lewes soil. For the Newark soil, approximately 11% of As was desorbed with 0.1 mM KH_2PO_4, and 70% was desorbed with 1 mM KH_2PO_4. For the

Camden soil, approximately 20% of total As was desorbed with 0.1 mM KH_2PO_4, and 13% was desorbed with 1 mM KH_2PO_4.

Based on desorption studies, As is relatively immobile in these soils but has potential to be released with the application of P fertilizer. Phosphate and arsenate react very similarly in soils and compete for sorption sites on Fe and Al oxides (Neupane et al., 2014), and studies have shown increasing rates of As desorption from mineral surfaces when phosphate is introduced (Cui et al., 2013; Neupane et al., 2014). Peryea et al. (1991) also observed significant As desorption in studies reacting lead arsenate-contaminated soils with 1 mM monoammonium phosphate and monocalcium phosphate in batch reactions. They observed approximately 11% of total As desorbed after a 480 h for coarse loamy soils at pH 6.2.

Desorption studies reveal that As exchanges readily with phosphate, indicating that much of the soil As is present as adsorbed As species. The application of P fertilizers to As-contaminated sites may increase As transport, thereby increasing the potential for As to contaminate groundwater. It is essential to develop management recommendations for P fertilizer applications in Delaware former orchard soils if elevated levels of As are present. This is particularly important for soils in southern Delaware, since the sandy soils and high water tables in this region could accelerate the time required for As to reach groundwater.

4.3.3 Arsenic Bioavailability

Bioaccessible As concentrations averaged 4.74 mg kg^{-1} for the Lewes soil, 1.22 mg kg^{-1} for the Newark soil, and 0.35 mg kg^{-1} for the Camden soil (Table 4.3). Results indicate that no soil examined in this study contain greater than 22% relative bioavailable As (RBA), based on the upper limits for relative As bioavailability. These

results are in agreement with a review by Ruby et al. (1999), which showed an RBA

lower than 50% for 22 out of 24 soils contaminated with As from previous smelting and

mining activities. Bradham et al. (2011) observed less than 53% of total soil As to be

bioavailable in a study examining nine As-contaminated soils from previous smelting

and mining sites. The low pH and length of time since lead arsenate application for soils

in the current study may have contributed to an increase in As retention and decrease in

bioaccessibility. Yang et al. (2002) observed a significant decrease in As bioaccessibility

after six months in soils that had been spiked with As(V); the effect of aging on

decreasing bioaccessibility was even greater for low pH soils.

The Lewes soil at the 0-20 cm depth contained higher RBA than the Newark and

Camden soils. This is expected since the Lewes soil contained lower ammonium-oxalate

extractable (Fe + Al) than the Newark and Camden soils. The Lewes soil at the 0-20 cm

depth also has a higher pH than the Newark and Camden soils. Yang et al. (2002)

determined that Fe oxide content and pH are the two most important factors

controlling soil As bioaccessibility in a survey that examined the effect of Fe-oxide

content, Mn-oxide content, pH, CEC, carbonate content, organic C content, and particle

size on As retention in 36 soils containing a wide range of chemical and physical

properties. In addition to Fe oxide content and pH, Bradham et al. (2011) also observed

that total Fe and Al content had a large impact on bioaccessible As.

Results from bioavailability studies demonstrate that the majority of total As

remains insoluble during *in vitro* extractions, similar to results for As removal during

desorption with 10 mM KCl electrolyte solution. Conversely, desorption with phosphate

solutions resulted in release of 13 to 70% of total As. Combined data from desorption

and bioavailability studies support the conclusion that the majority of As in these soils is

bound through inner-sphere complexation, and As is primarily exchanged through

ligand exchange with phosphate. Arsenic which was not removed with *in vitro* extractions likely does not pose risk to human health. If the remediation standards for Delaware were based on RBA, no soils used in this study would fall above Delaware cleanup levels of 11 mg kg^{-1}. However, it should be noted that the Lewes and Newark soils would fall above the EPA screening level of 0.4 mg kg^{-1} based on soil bioavailable As.

4.3.4   Arsenic Speciation

X-ray fluorescence and absorption analysis was performed on soils from the Lewes and Newark locations. X-ray fluorescence maps revealed that As in the former orchard soils is co-located with Fe at many hotspots (Fig 4.5, 4.6, 4.7, 4.8). Arsenic was heterogeneously distributed throughout soil samples. Heterogeneous distribution of As, with some As hotspots occurring in diffuse, low concentration areas and some hotspots occurring in localized high concentration, is a common observation (Arai et al., 2006; Landrot et al., 2012).

The absorption edge for the As(V) mineral standard was present at approximately 11876 eV (Fig 4.5). For sorbed As(III), there is a 3-4 eV downward shift relative to that of As(V) to 11872 eV. As sulfide mineral resulted in a further shift downward to the absorption edge of approximately 11870 eV. All hotspots measured for the Lewes site indicate the As is present in the As(V), the less mobile and toxic, form (Fig. 4.5 and 4.6). Pronounced secondary features in As K-edge XANES spectra indicate that a crystalline mineral species is associated with As (Landrot et al, 2012). The pronounced secondary peak present at approximately 11882 eV indicate that As is associated with a crystalline mineral species for Point 3 in the Lewes 0-20 cm sample

and Point 1 in the Lewes 20-40 cm sample. The majority of XANES spectra do not contain such features and are likely sorbed species of As.

Spectra collected for the As hotspots at the Newark location also indicate that As is predominately in the As(V) form (Fig 4.7 and Fig 4.8). Seven of these eight hotspots were present in the As(V) form. One hotspot, Newark 0-20_Point 1 appeared to be an As(III) sulfide species. Even in oxic soils, small amounts of soil As(V) can reduce to As(III) (Cui and Weng, 2013). One hotspot, Newark 0-20_Point 2, contained a secondary feature at 11897 eV which indicates As is associated with a crystalline mineral.

Out of 19 As hotspots examined for the Lewes and Newark soils, only one As hotspot appeared to be in the As(III) form. This was expected for the oxic, sandy soils assessed in this study and is in accordance with Arai et al. (2006), who used synchrotron-based X-ray techniques to determine that As was primarily present as As(V) sorbed to amorphous Fe oxides at a heavily-contaminated site (284 mg As kg^{-1} soil) which had previously contained a lead arsenate production company. Arai et al. (2006) also observed the presence of As sulfide species in a soil sample collected from a contaminated site under semi-reducing conditions.

The combination of XRF, XANES, and desorption data indicate that As is primarily bound to Fe- and Al-oxide species. Results from bulk soil characterization, which show the presence of ammonium-oxalate extractable Fe and Al, support this conclusion. Even at low concentrations, Fe- and Al-oxides are important contributors to As retention in soils due to their large surface area and reactivity. Co-location of Fe and As was observed for many As hotspots. Although it was not possible to map Al at the incident X-ray energy used for XRF mapping, it is likely that many As hotspots correspond with Al hotspots. Landrot et al. (2012) observed that As was primarily associated with Al, either as As sorbed to Al oxide or as an As-Al mineral, in Delaware contaminated soils. Iron-

and Al- oxides have a high affinity to sorb and strongly retain arsenate via inner sphere complexation (Fendorf et al., 1997; Arai et al.,2005; Neupane et al., 2014). A few hotspots of As appear to be in crystalline mineral form based on pronounced secondary peak features. Speciation results indicate that As is in its less-toxic oxidation state, As(V), and is strongly sorbed by Fe- and Al-oxides in soils; these forms of As are likely to have minimal environmental impact in unaltered soils.

4.4   Conclusions

Arsenic retention in former orchard soils is dependent on many soil chemical conditions including pH, OM content, mineralogy, and presence of competing ions in solution. Desorption studies show that As is strongly retained in background electrolyte solution, but increasing concentration of competing ions, especially phosphate, increases the release of As. Therefore, P fertilizer application has potential to increase As mobility in historically-contaminated orchard soils. Bioaccessibility studies demonstrate that total soil As in former orchard soils may not be representative of As that is bioavailable to humans. Less than 22% of total As is considered bioavailable at all previous orchard locations. Based on this data, we suggest that priority for site remediation of be given to historically-contaminated orchard sites with the highest relative bioavailable As concentrations, particularly for soils with > 11 ppm relative bioaccessible As. For residential sites where remediation may not be priority, bare soil can be covered with ornamental turf, mulch, or landscape fabric to minimize human exposure to As. Arsenic in soils examined for this study was primarily present in the As(V) form, which is less mobile and toxic than As(III), based on synchrotron-based X-ray analysis. Speciation analysis combined with desorption data indicate that the majority of soil As is sorbed to Fe- and Al- oxides at historically-contaminated orchard sites. It is

important to note that As is not homogeneously distributed at former orchard sites. Increased As concentrations may exist in areas of former orchards where higher rates of lead arsenate were applied or areas where pesticide was disposed. Considerations for remediation should be site-specific, as soil type, land use, and water table depth will have a significant effect on As transport in the environment.

Table 4.1. Soil characterization analysis of former orchard soils in Delaware and control soils.

Location	Depth	pH	OM[1]	CEC[2]	Total Al	Total Fe	Al_{ox}[3]	Fe_{ox}[4]	Sand	Silt	Clay
	cm		g kg^{-1} soil	meq 100 g^{-1}	—— g kg^{-1} soil ——		—— mg kg^{-1} soil ——		——— % ———		
Lewes	0-20	6.2	10.7	4.9	11.74	8.13	1002.9	707.5	30	52	18
	20-40	5.7	8.7	3.7	11.35	8.37	875.6	639.8	46	36	18
Newark	0-20	5.7	21.3	7.8	19.05	18.42	1291.5	2132.5	8	66	26
	20-40	5.8	22.7	7.7	17.18	17.23	1488.4	2364.9	6	68	26
Camden	0-20	5.6	13.7	5.1	9.90	7.79	1259.5	780.7	63	27	10
	20-40	5.9	7.0	3.9	13.02	9.48	1958.4	793.5	62	15	23
Felton	0-20	5.9	12.5	4.8	8.79	4.92	864.2	628.5	70	20	10
	20-40	6.2	10.5	3.8	10.86	5.94	1627.5	711.0	70	20	10
Lincoln	0-20	5.9	7.0	3.3	5.83	2.60	336.3	407.2	78	15	7

[1] Organic matter content

[2] Cation exchange capacity

[3] Ammonium-oxalate extractable Al

[4] Ammonium-oxalate extractable Fe

Table 4.2. Mehlich-3 extractable element concentrations for former orchard soils and control soils.

Location	Depth	Mehlich3-Extractable Elements										
		P	K	Ca	Mg	Mn	Zn	Cu	Fe	B	S	Al
	cm	—————————————————————— mg kg^{-1} soil ——————————————————————										
Lewes	0-20	69.0	156.0	490.3	140.5	30.2	3.5	7.2	92.5	0.36	15.9	970.9
	20-40	47.1	96.5	291.3	102.2	22.3	2.5	7.0	99.6	0.26	18.0	1122.7
Newark	0-20	89.4	150.8	834.4	217.5	50.4	3.4	3.1	124.0	0.25	11.0	1005.4
	20-40	89.3	168.0	828.8	218.1	47.9	3.6	3.3	123.1	0.28	12.3	963.9
Camden	0-20	20.4	63.2	454.5	87.0	9.7	3.4	1.3	67.2	0.24	6.7	585.3
	20-40	19.2	57.4	334.1	71.6	9.7	1.8	1.5	65.8	0.14	5.5	673.4
Felton	0-20	61.7	105.1	575.7	122.2	35.2	3.2	1.8	84.2	0.33	13.6	840.7
	20-40	60.8	69.4	446.7	95.7	29.7	2.6	2.3	85.8	0.22	13.0	927.6
Lincoln	0-20	63.9	84.3	348.8	70.9	14.1	2.1	1.5	79.0	0.13	14.0	764.3

Table 4.3. Total As, total Pb, As:Pb ratio, bioaccessible As concentrations, and percent

bioavailable As in old orchard soils and control soils.

Location	Depth	Total As	Total Pb	As:Pb Ratio	Bioaccessible As	Bioavailable As
	cm	——— mg kg^{-1} ———			—— mg kg^{-1} ——	—— % ——
Lewes	0-20	40.1 ± 4.5	112.0 ± 3.9	0.36	4.74 ± 2.36	13.2 ± 8.1
	20-40	59.0 ± 5.7	116.5 ± 8.7	0.51	3.85 ± 2.53	10.7 ± 8.0
Newark	0-20	23.6 ± 1.8	66.7 ± 2.6	0.35	1.22 ± 0.04	7.9 ± 3.2
	20-40	26.5 ± 2.1	63.1 ± 6.2	0.42	1.27 ± 0.12	8.1 ± 3.5
Camden	0-20	11.8 ± 2.1	25.9 ± 1.5	0.46	0.35 ± 0.09	6.0 ± 3.8
	20-40	13.8 ± 0.7	38.1 ± 11.8	0.36	0.48 ± 0.16	7.5 ±4.5
Felton	0-20	5.5 ± 0.3	8.0 ± 0.7	0.69	0.24 ± 0.05	7.2 ± 3.8
	20-40	3.9 ± 0.6	7.8 ± 0.5	0.49	0.32 ± 0.49	8.8 ± 11.9
Lincoln	0-20	1.4 ± 0.1	6.8 ± 0.5	0.20	0.00 ± 0.00	0.0 ± 0.0

Figure 4.1. Aerial Photograph from 1937 of former orchard site in Lewes, DE.

Figure 4.2. Aerial Photograph from 1937 of former orchard site in Newark, DE.
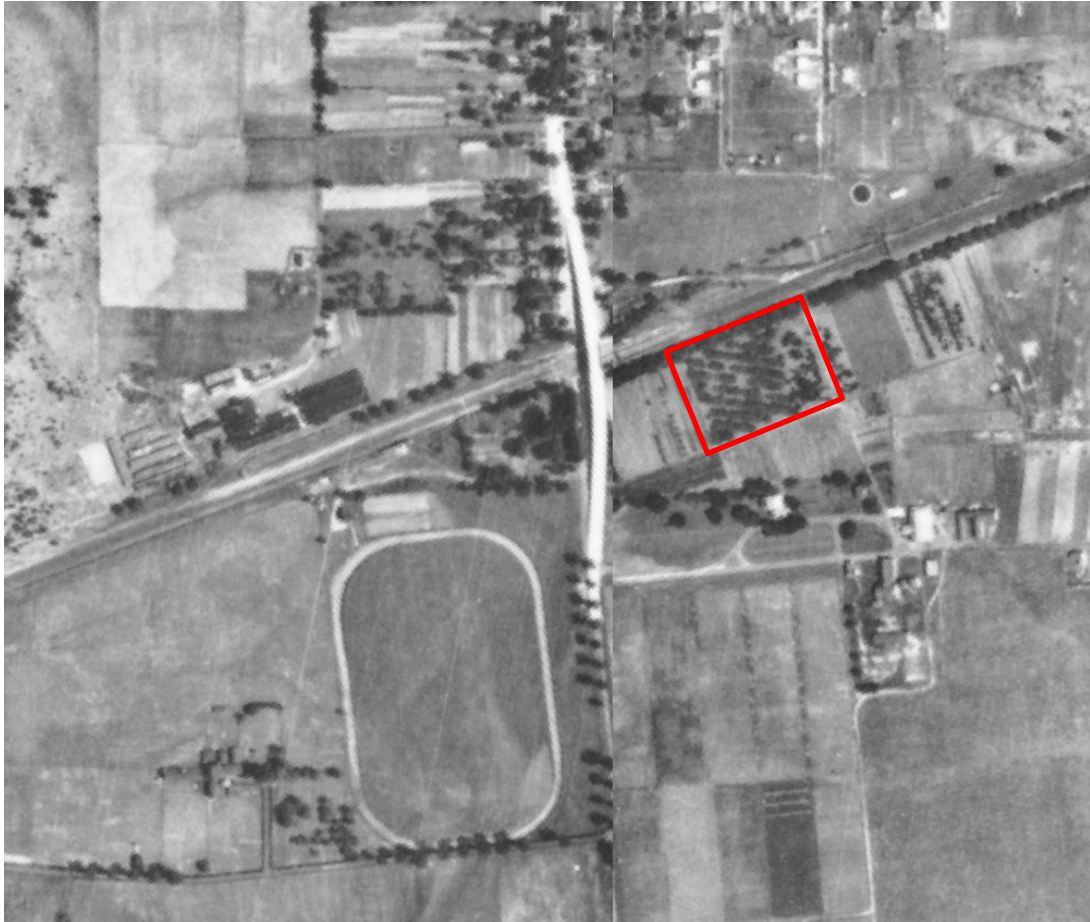
Figure 4.3. Aerial Photograph from 1937 of former orchard site in Camden, DE.

Figure 4.4. Arsenic release over a 24-h desorption experiment in 10 mM KCl, 0.1 mM

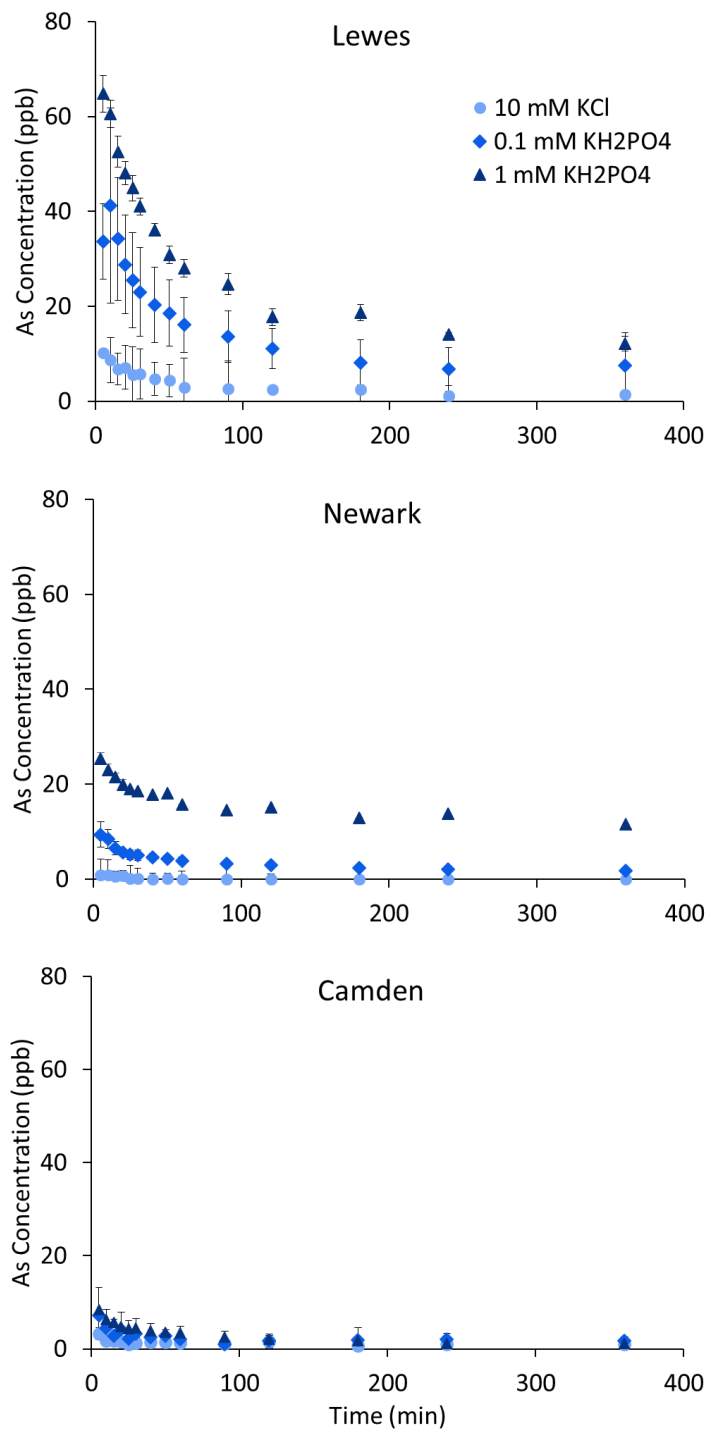KH_2PO_4, and 1 mM KH_2PO_4 for Lewes, Newark, and Camden soils.

Figure 4.5. Micro-XRF image of old orchard soil from Lewes, DE, at the 0-20 cm depth showing elemental distribution of As (red) and Fe (blue) and corresponding XANES spectra.
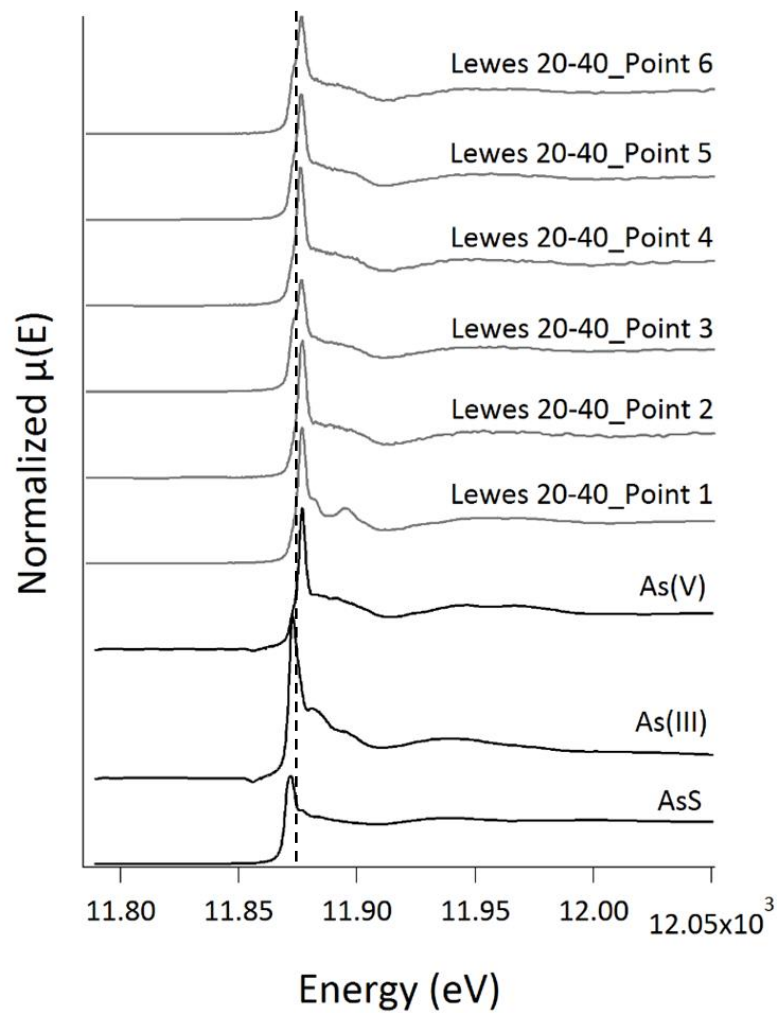
93
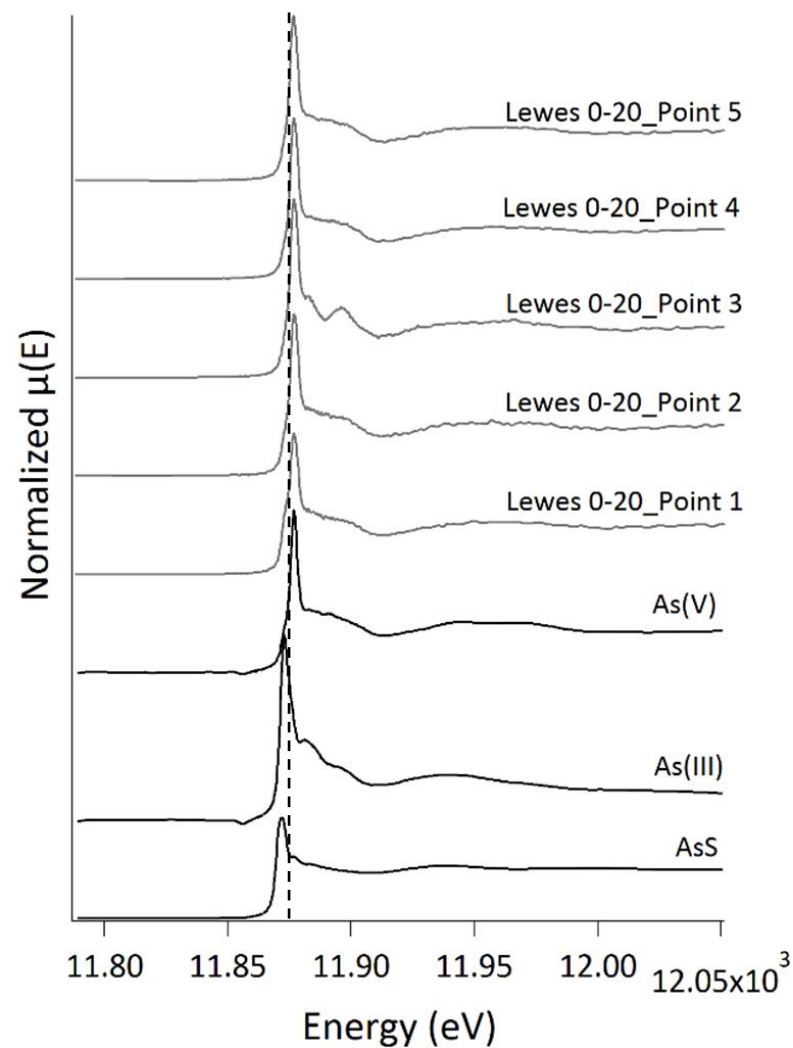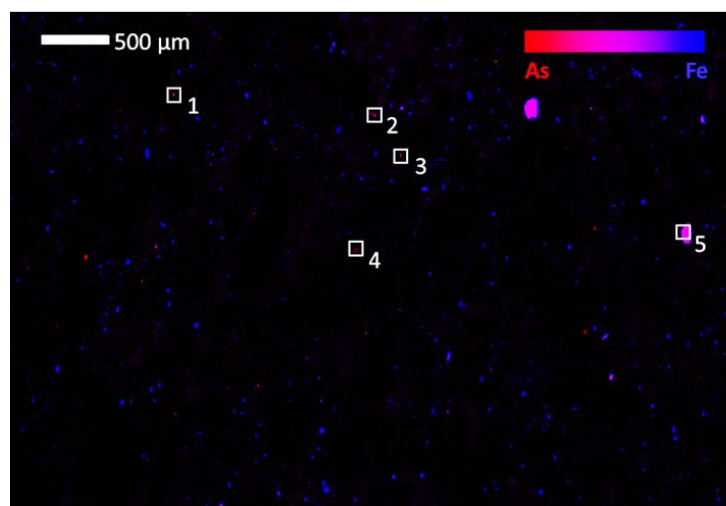
Figure 4.6. Micro-XRF image of old orchard soil from Lewes, DE, at the 20-40 cm depth showing elemental distribution of As (red) and Fe (blue) and corresponding XANES spectra.
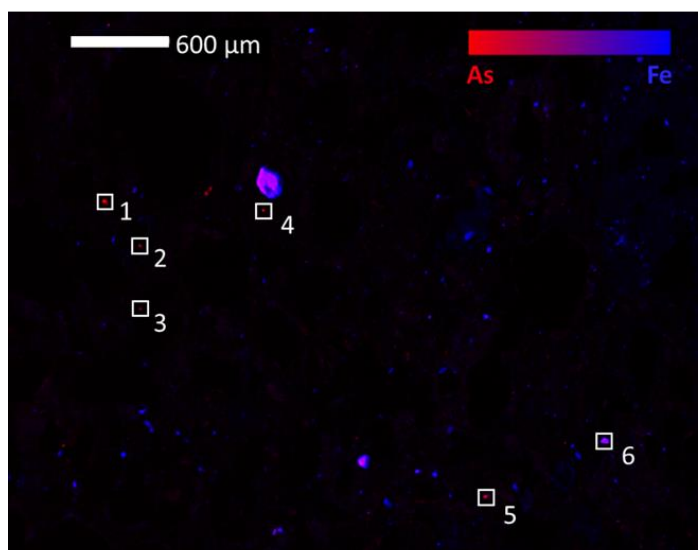
Figure 4.7. Micro-XRF image of old orchard soil from Newark, DE, at the 0-20 cm depth showing elemental distribution of As (red) and Fe (blue) and corresponding XANES spectra.
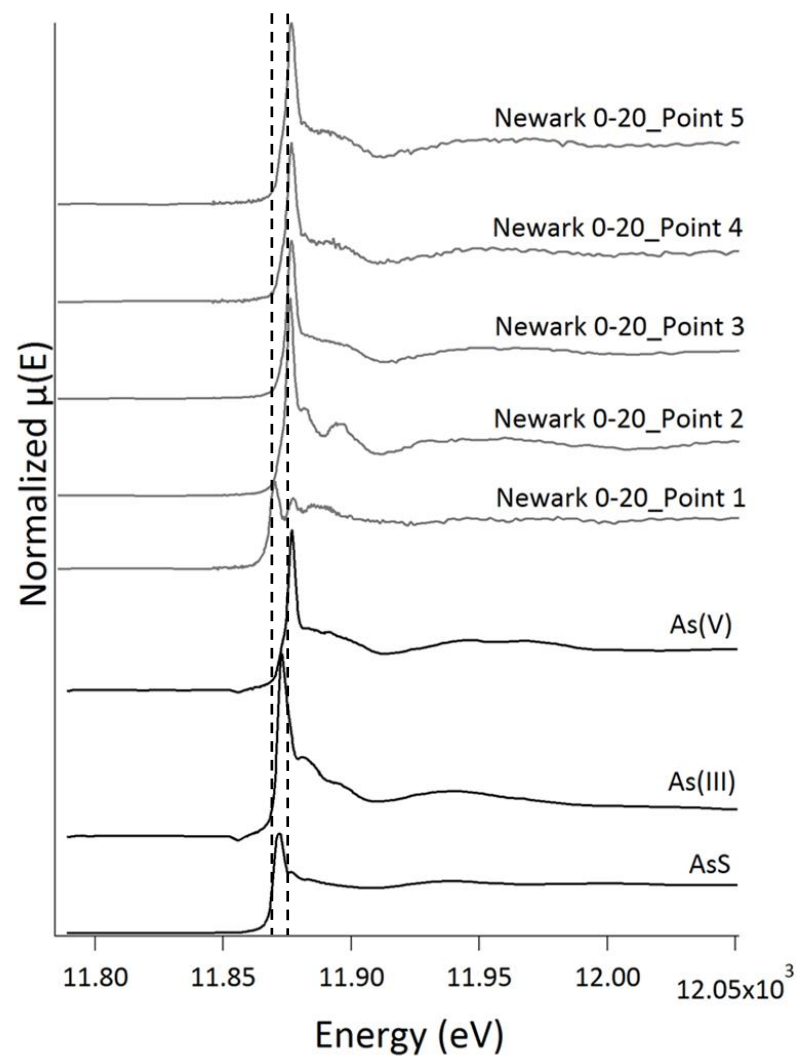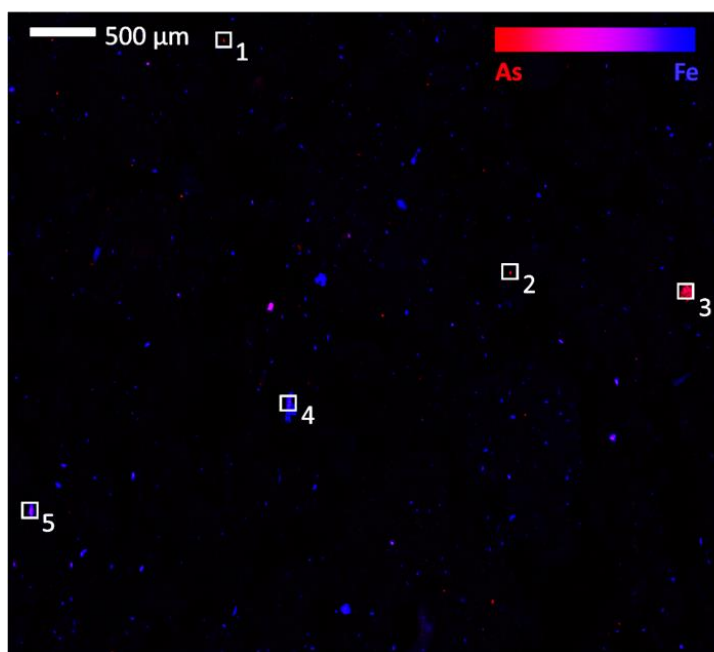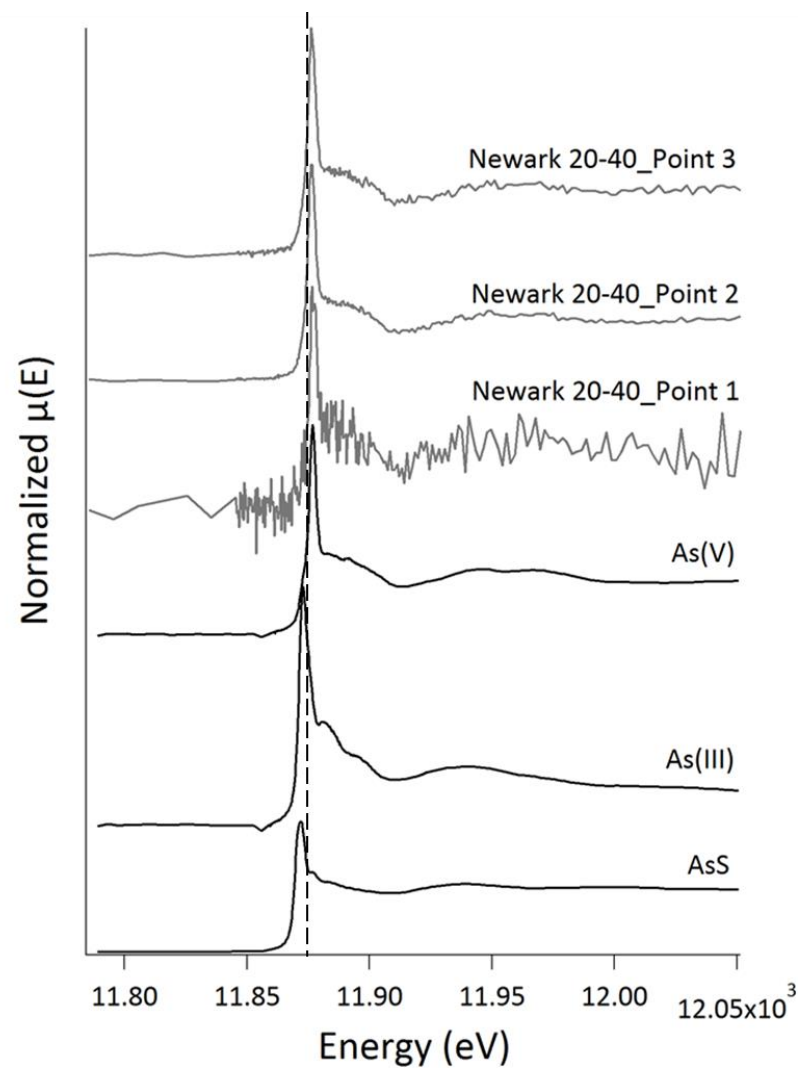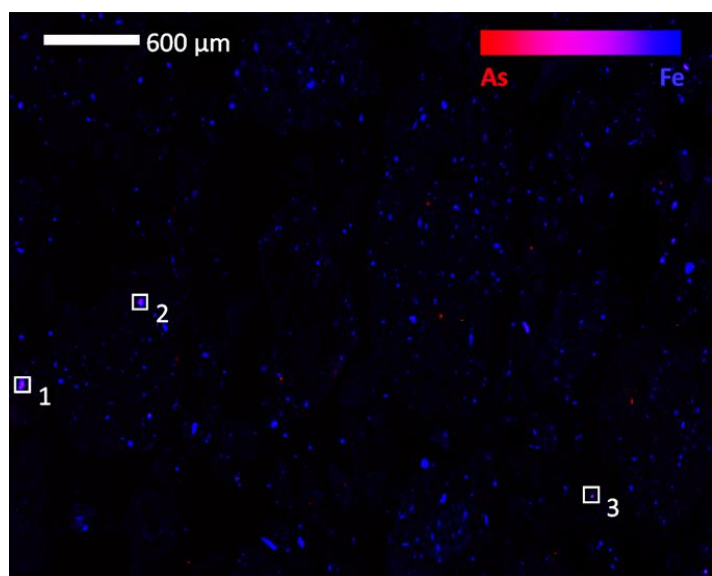
Figure 4.8. Micro-XRF image of old orchard soil from Newark, DE, at the 20-40 cm depth showing elemental distribution of As (red) and Fe (blue) and corresponding XANES spectra.

REFERENCES

Abdala, D.B., I. Ribeiro de Silva, L. Vergütz, and D.L. Sparks. 2015. Long-term manure application effects on phosphorous speciation, kinetics, and distribution in highly weathered agricultural soils. Chemosphere. 119:504-514.

Arai, Y., D.L. Sparks, and J.A. Davis. 2005. Arsenate adsorption mechanisms at the allophane-water interface. Environ. Sci. Technol. 39:2537-2544.

Arai, Y., and D.L. Sparks. 2007. Phosphate reaction dynamics in soils and soil components: a multiscale approach. Adv Agron. 94:135-179.

Arai, Y., A. Lanzirotti, S.R. Sutton, M. Newville, J. Dyer, and D.L. Sparks. 2006. Spatial and temporal variability of arsenic solid-state speciation in historically lead arsenate contaminated soils. Environ. Sci. Technol. 40:673-679.

Beak, D.G., N.T. Basta, K.G. Scheckel, and S.L. Traina. 2006. Bioaccessibility of arsenic(V) bound to ferrihydrite using a simulated gastrointestinal system. Environ. Sci. Technol. 40:1364-1370.

Bradham, K.D., K.G. Scheckel, C.M. Nelson, P.E. Seales, G.E. Lee, M.F. Hughes, B.W. Miller, A. Yeow, T. Gilmore, S.M. Serda, S. Harper, and D.J. Thomas. 2011. Relative bioavailability and bioaccessibility and speciation of arsenic in contaminated soils. Environ. Health Persp. 119:1629-1634.

Cui, Y. and L. Weng. 2013. Arsenate and phosphate adsorption in relation to oxides composition in soils: LCD modeling. Environ. Sci. Technol. 47:7269-7276.

Davenport, J.R., and F.J. Peryea. 1991. Phosphate fertilizers influence leaching of lead and arsenic in a soil contaminated with lead arsenate. Water Air Soil Poll. 57-58:101-110.

Delaware Environmental Monitoring Analysis Center. 2016. Delaware Aerial Data Distribution. Available online http://demac.udel.edu/tiles/. Accessed [12/11/2016].

Department of Natural Resources and Environmental Control (DNREC). 2007. Arsenic risk management plan background document.

Diamond, G.L., K.D. Bradham, W.J. Brattin, M. Burgess, S. Griffin, C.A. Hawkins, A.L. Juhasz, J.M. Klotzbach, C. Nelson, Y.W. Lowney, K.G. Scheckel, and D.J. Thomas. 2016. Predicting oral relative bioavailability of arsenic in soil from in vitro bioaccessibility. J. Toxicol. Env. Heal. A. 79:165-173.

Dixit, S. and J.G. Hering. 2003. Comparison of arsenic(V) and arsenic(III) sorption onto iron oxide minerals: implications for arsenic mobility. Environ. Sci. Technol. 37:4182-4189.

Environmental Protection Agency (EPA). 1995. EPA method 3050b: Acid digestion of sediments, sludges, and soils. In Test Methods for Evaluating Solid Waste, 3rd update. United States Environmental Protection Agency, Washington, D.C.

Fendorf, S., M.J. Eick, P. Grossl, and D.L. Sparks. 1997. Arsenate and chromate retention mechanisms on goethite. 1. Surface structure. Environ. Sci. Technol. 31:315-320.

Hedrick, U.P., G.H. Howe, O.M. Taylor, and C.B. Tubergen. 1917. The peaches of New York. New York Agric. Expt. Stn. J.B. Lyon Publishers, Albany, NY.

Jackson, M.L., C.L. Lim, and L.W. Zelzany. 1986. Oxides, hydroxides, and aluminosilicates. pg. 101-150. In A. Klute (ed.) Methods of Soil Analysis. Part 1. SSSA and ASA, Madison, WI.

Jones, J.S., and M.B. Hatch. 1937. The significance of inorganic spray residue accumulations in orchard soils. Soil Sci. 44:37-64.

Lafferty, B.J., M. Ginder-Vogel, and D.L. Sparks. 2011. Arsenite oxidation by a poorly-crystalline manganese oxide. 3. Arsenic and manganese desorption. Env. Sci. Technol. 45:9218-9223.

Landrot, G., R. Tappero, S.M. Webb, and D.L. Sparks. 2012. Arsenic and chromium speciation in an urban contaminated soil. Chemosphere. 88:1196-1201.

Merry, R.H., K.G. Tiller, and A.M. Alston. 1983. Accumulation of copper, lead, and arsenic in some Australian orchard soils. Aust. J. Soil. Res. 21:549-561.

Merwin, I., P.T. Pruyne, J.G. Ebel, K.L. Manzell, and D.J. Lisk. 1994. Persistence, phytotoxicity, and management of lead, arsenic, and mercury residues in old orchard soils of New York State. Chemosphere. 29:1361-1367.

Neupane, G., R.J. Donahoe, Y. Arai. 2014. Kinetics of competitive adsorption/desorption of arsenate and phosphate at the ferrihydrite-water interface. Chemical Geol. 368:31-38.

Peryea, F.J. 1991. Phosphate-induced release of arsenic from soils contaminated with lead arsenate. Soil Sci. Soc. Am. J. 55:1301-1306.

Peryea, F.J. 1998. Phosphate starter fertilizer temporarily enhances soil arsenic uptake by apple trees grown under field conditions. Hort. Sci. 33:826-829.

Peryea, F.J. and T.L. Creger. 1994. Vertical distribution of lead and arsenic in soils contaminated with lead arsenate pesticide residues. Water Air Soil Poll. 78:297-306.

Ravel, B., and M. Newville. 2005. Athena, Artemis, Hephaestus: Data analysis for x ray absorption spectroscopy using IFEFFIT. J. Synchrotron Radiat. 12:537 541.

Raven, K.P., A. Jain, and R.H. Loeppert. 1998. Arsenite and arsenate adsorption on ferrihydrite: Kinetics, equilibrium, and adsorption envelopes. Environ. Sci. Technol. 32:344-349.

Ruby, M.V., R Schoof, W. Brattin, M. Goldade, G. Post, M. Harnois, D.E. Mosby, S.W. Casteel, W. Berti, M. Carpentier, D. Edwards, D. Cragin, and W. Chappell. 1999. Advances in evaluating the oral bioavailability in soil for use in human health risk assessment. Env. Sci. Technol. 33:3697-3705.

Scheckel, K.G., C.A. Impelletteri, J.A. Ryan, and T. McEvoy. 2003. Assessment of a sequential extraction procedure for perturbed lead-contaminated samples with and without phosphorus amendments. Environ. Sci. Technol. 37:1892-1898.

Scheckel, K.G., R.L. Chaney, N.T. Basta, and J.A. Ryan. 2009. Advances in assessing bioavailability of metal(loid)s in contaminated soils. Adv. Agron. 104:1-52.

Shacklette, H.T. and J.G. Boerngen. 1984. Element concentrations in soils and other surficial materials of the conterminous United States. United States Government Printing Office, Washington DC.

Sims, J.T., R.O. Maguire, A.B. Leytem, K.L. Gartley, and M.C. Pautler. 2002. Evaluation of Mehlich 3 as an agri-environmental soil phosphorous test for the mid-Atlantic United States of America. Soil Sci. Soc. Am. J. 66:2016-2032.

Sims, J.T. and A. Wolf. 2011. Recommended soil testing procedures for the northeastern United States. Northeast Regional Bulletin 493. Agricultural Experiment Station, University of Delaware, Newark, DE.

Sparks, D.L., S.E. Fendorf, C.V. Toner, and T.H. Carski. 1996. Kinetic methods and measurements. In: D.L. Sparks (ed.) Methods of Soil Analysis: Part 3. SSSA and ASA, Madison, WI.

Udovic, M., and M.B. McBride. 2012. Influence of compost addition on lead and arsenic bioavailability in reclaimed orchard soil using Porcellio scaber bioaccumulation test. J. Hazard. Mater. 205-206:144-149.

USDA-NRCS. 2016. Web Soil Survey. Available online at
http://websoilsurvey.nrcs.usda.gov/. Accessed [03/10/2017].

Webb, S.M. 2005. SIXpack: A graphical user interface for XAS analysis using IFEFFIT.
Physica Scripta. T115:1011-1014.

Yang, J., M.O. Bennett, P.M. Jardine, N.T. Basta, and S.W. Casteel. 2002. Adsorption,
sequestration, and bioaccessibility of As(V) in soils. Environ. Sci. Technol.
36:4562-4569.

Appendix

PRELIMINARY X-RAY FLUORESCENCE MAPS FROM THE TES (TENDER ENERGY SPECTROSCOPY) BEAMLINE AT NSLS-II (NATIONAL SYNCHROTRON LIGHT SOURCE II)

X-ray fluorescence (XRF) images (3 mm x 3 mm) of Si (top left), P (top right), S, (bottom left) Mg (bottom right) for the Mullica-Berryland soil. For the XRF maps, the incident energy is 2575 eV, beam spot-size is approximately 10 um vertical x 40 um horizontal, and pixel size 15 um x 15 um. Regions with high-intensity Si show quartz grains; lower-intensity grains are a likely a different mineral or clay. Phosphorus is primarily located in small hotspots. Sulfur hotspots may indicate the presence of organic matter. Mg indicates other minerals.